Wakefield Acceleration Based on Smith-Purcell Effect in Corrugated Dielectric Capillary

Alexey Tishchenko[1,2], Aleksandr Pomomarenko[1,2], Konstantin Lekomtsev[3], Daria Sergeeva[1,2], Aleksandr Aryshev[4], Mikhail Strikhanov[1], Aleksey Lyapin[3], Stiven Boogert[3], Nobuhiro Terunuma[4], Junji Urakawa[4]

[1]National Research Nuclear University "MEPhI", Moscow

[2]National Research Center "Kurchatov Institute", Moscow

[3]John Adams Institute at Royal Holloway University of London, Egham, UK

[4]High Energy Accelerator Research Organization KEK, Tsukuba, Japan

23-29 September, Channeling 2018, Ischia, Italia

Outline

- **Motivation**
- **Layout – capillary with periodical internal radii (SPR + CR)**
- **SPR for wakefield acceleration**

\- *Experiment **LUCX, KEK** (2016-2018)*

\- *Theoretical results*

\- *Vsim simulation (new experiment LUCX - 2018)*

- **Summary and plans**

Motivation

- There is urgent need to develop new acceleration techniques capable of exceeding hundred of MeV/m or GeV/m gradients in order to enable future generations of light sources and high-energy physics experiments
- Gradients in order of 100 MeV/m have been achieved by conventional techniques
- The enabling acceleration technology must feature high effective gradient, high efficiency, low fabrication cost, small sizes
- Dielectric Wakefield Accelerators (DWA) - intense relativistic electron beam is accelerated directly into the accelerator structure by high intense wakefields
- DWAs typically operate in the terahertz frequency range, which pushes the plasma breakdown threshold for surface electric fields into the multi GeV/m range

B.O'Shea et all, Observation of acceleration and deceleration in gigaelectron-voltper-metre gradient dielectric wakefield accelerators, Nat. Commun. 7, 12763 (2016)

Dielectric Wakefield Accelerators (DWA)

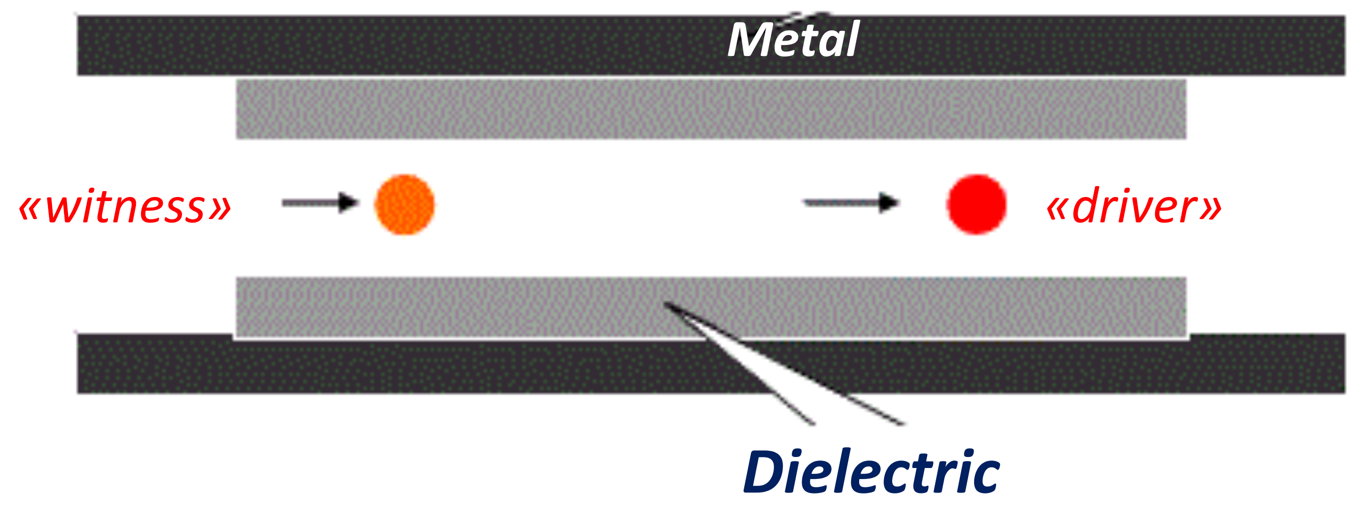

***DWA** usually based on **Cerenkov radiation** mechanism!*

We investigate DWA** based on **Smith-Purcell (SPR)!

SPR:

$$\frac{d}{\lambda}\left(\cos\theta-\left(\beta\sqrt{\varepsilon}\right)^{-1}\right)=n$$

$$n=1,2,3\ldots,-1,-2$$

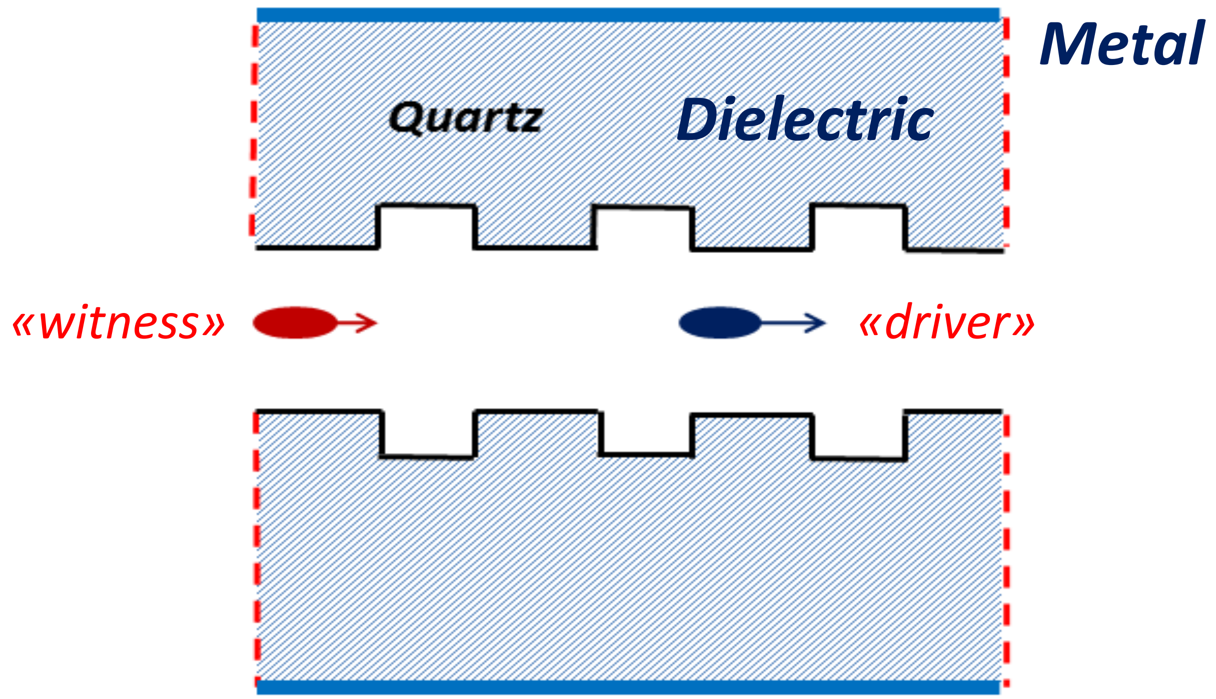

Experiment – LUCX, KEK, Japan

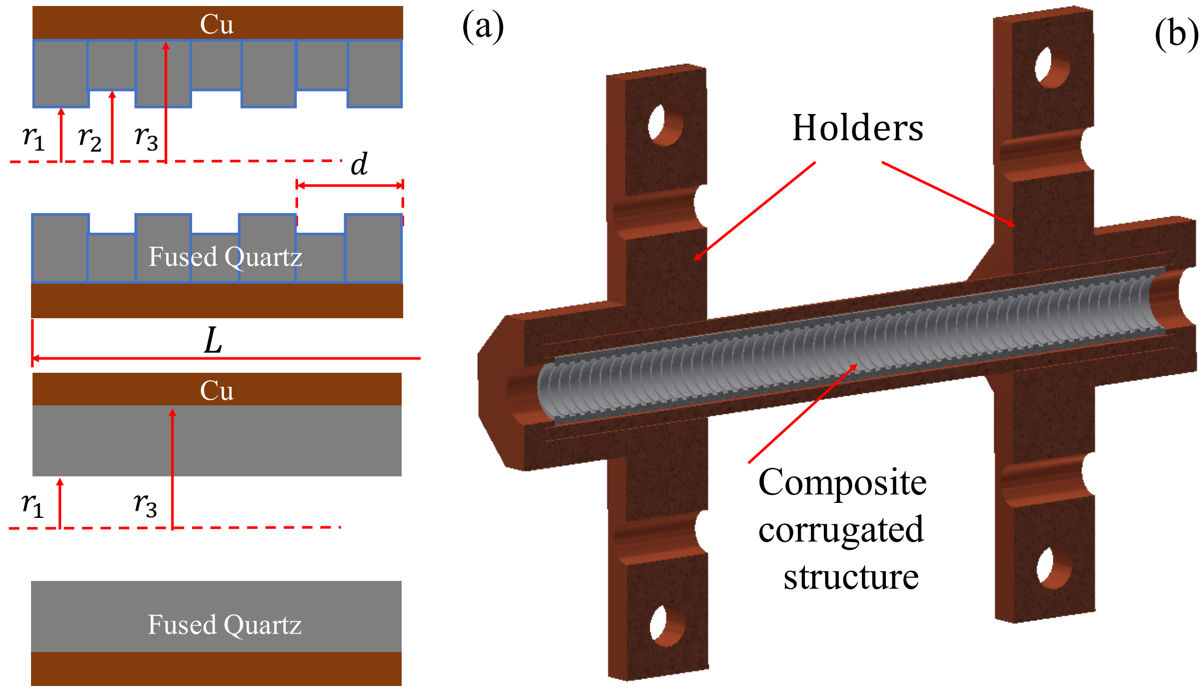

Parameter	Value
Drive bunch charge Q_{dr}	20 pC
Witness bunch charge Q_{w}	$\approx Q_{\mathrm{dr}}/3$
Drive bunch $\sigma^{\mathrm{dr}}_{\mathrm{transv}}$	230 μm
Witness bunch $\sigma^{\mathrm{w}}_{\mathrm{transv}}$	90 μm
Drive bunch $\sigma^{\mathrm{dr}}_{\mathrm{long}}$	0.5 ps (0.15 mm)
Witness bunch $\sigma^{\mathrm{w}}_{\mathrm{long}}$	0.35 ps (0.105 mm)
Repetition rate, max	3.13 bunch/s
Normalised emittance, typical	1.5×1.5 mm mrad
Drive-to-Witness separation	1.6 – 3.4 mm
Capillary length, L	60 mm
Capillary material	Fused Quartz
r_1; r_2; r_3	2; 2.2; 2.7 mm
Corrugation period, d	1 mm

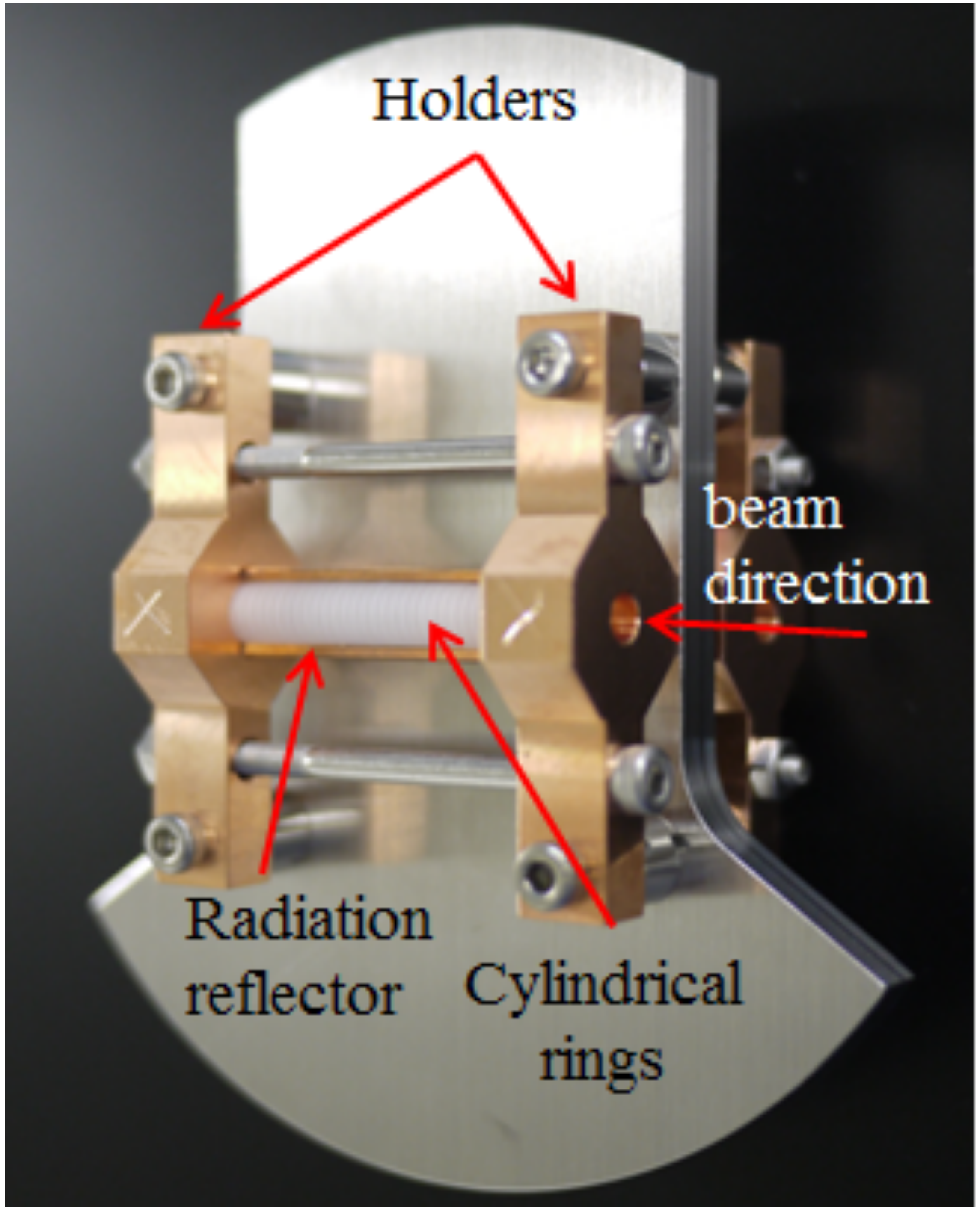

Experiment №1 – LUCX, KEK, Japan

Sub-THz radiation from dielectric capillaries with reflectors

K. Lekomtsev [a,*], A. Aryshev [b], A.A. Tishchenko [c], M. Shevelev [b], A.A. Ponomarenko [c], P. Karataev [a], N. Terunuma [b,d], J. Urakawa [b]

[a] *John Adams Institute at Royal Holloway University of London, Egham, Surrey TW20 0EX, UK*
[b] *KEK: High Energy Accelerator Research Organization, 1-1 Oho, Tsukuba, Ibaraki 305-0801, Japan*
[c] *National Research Nuclear University MEPhI, Kashirskoe sh. 31, Moscow 116409, Russia*
[d] *SOKENDAI: The Graduate University for Advanced Studies, 1-1 Oho, Tsukuba, Ibaraki 305-0801, Japan*

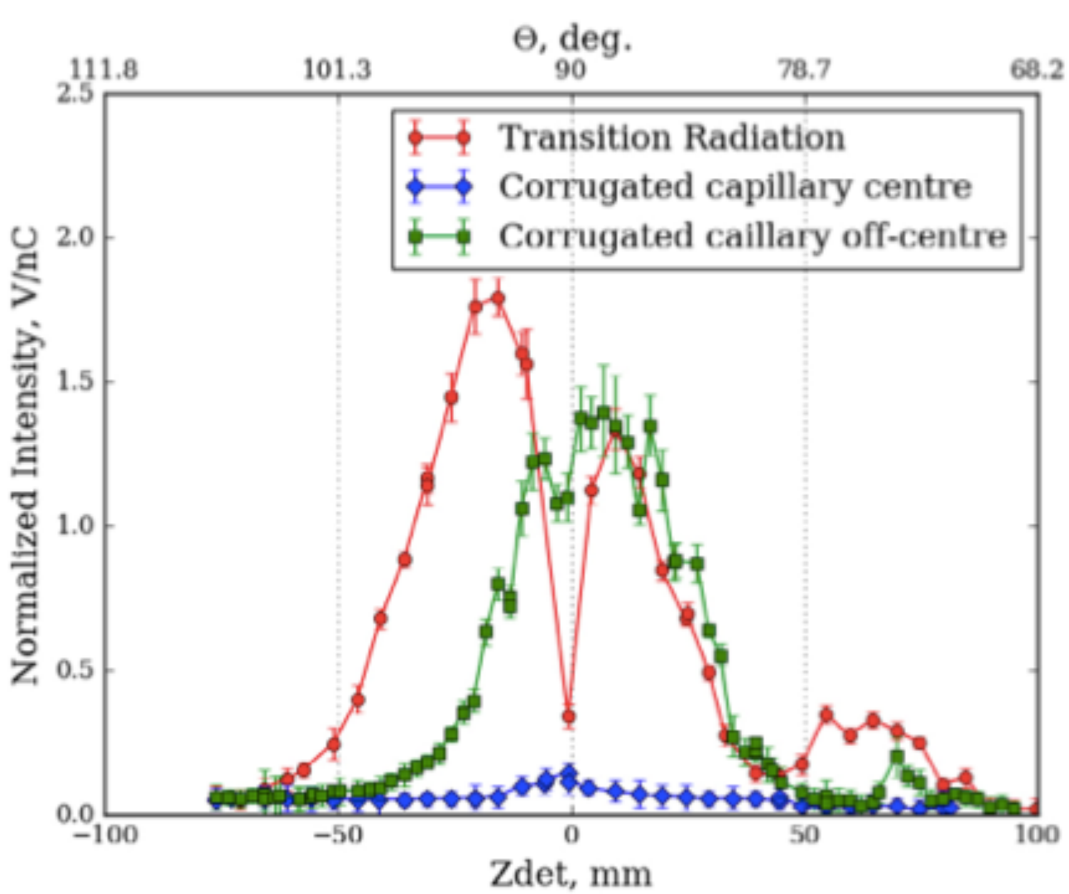

Fig. 2. Crosscheck with Transition Radiation.

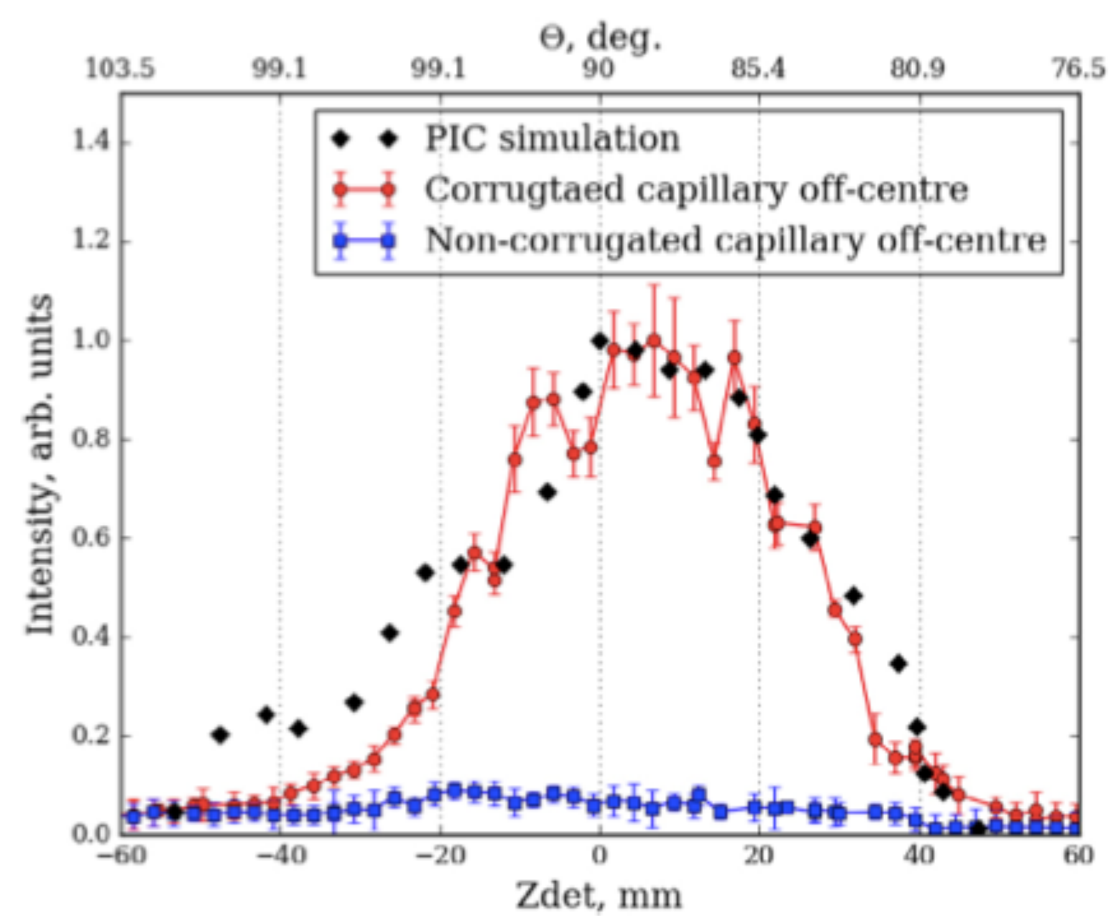

Fig. 3. Radiation distribution along axis z. (For interpretation of the references to colour in this figure legend, the reader is referred to the web version of this article.)

Experiment №2 – LUCX, KEK, Japan

PHYSICAL REVIEW ACCELERATORS AND BEAMS **21**, 051301 (2018)

Driver-witness electron beam acceleration in dielectric mm-scale capillaries

K. Lekomtsev,[1,*] A. Aryshev,[2,3] A. A. Tishchenko,[4,5] M. Shevelev,[6] A. Lyapin,[1] S. Boogert,[1] P. Karataev,[1] N. Terunuma,[2,3] and J. Urakawa[2]

Parameter	Value
Drive bunch charge Q_{dr}	20 pC
Witness bunch charge Q_{w}	$\approx Q_{\mathrm{dr}}/3$
Drive bunch $\sigma^{\mathrm{dr}}_{\mathrm{transv}}$	230 μm
Witness bunch $\sigma^{\mathrm{w}}_{\mathrm{transv}}$	90 μm
Drive bunch $\sigma^{\mathrm{dr}}_{\mathrm{long}}$	0.5 ps (0.15 mm)
Witness bunch $\sigma^{\mathrm{w}}_{\mathrm{long}}$	0.35 ps (0.105 mm)
Repetition rate, max	3.13 bunch/s
Normalised emittance, typical	1.5×1.5 mm mrad
Drive-to-Witness separation	1.6 – 3.4 mm
Capillary length, L	60 mm
Capillary material	Fused Quartz
r_1; r_2; r_3	2; 2.2; 2.7 mm
Corrugation period, d	1 mm

Acceleration 170 keV/m

Layout №1 – E(r,t)

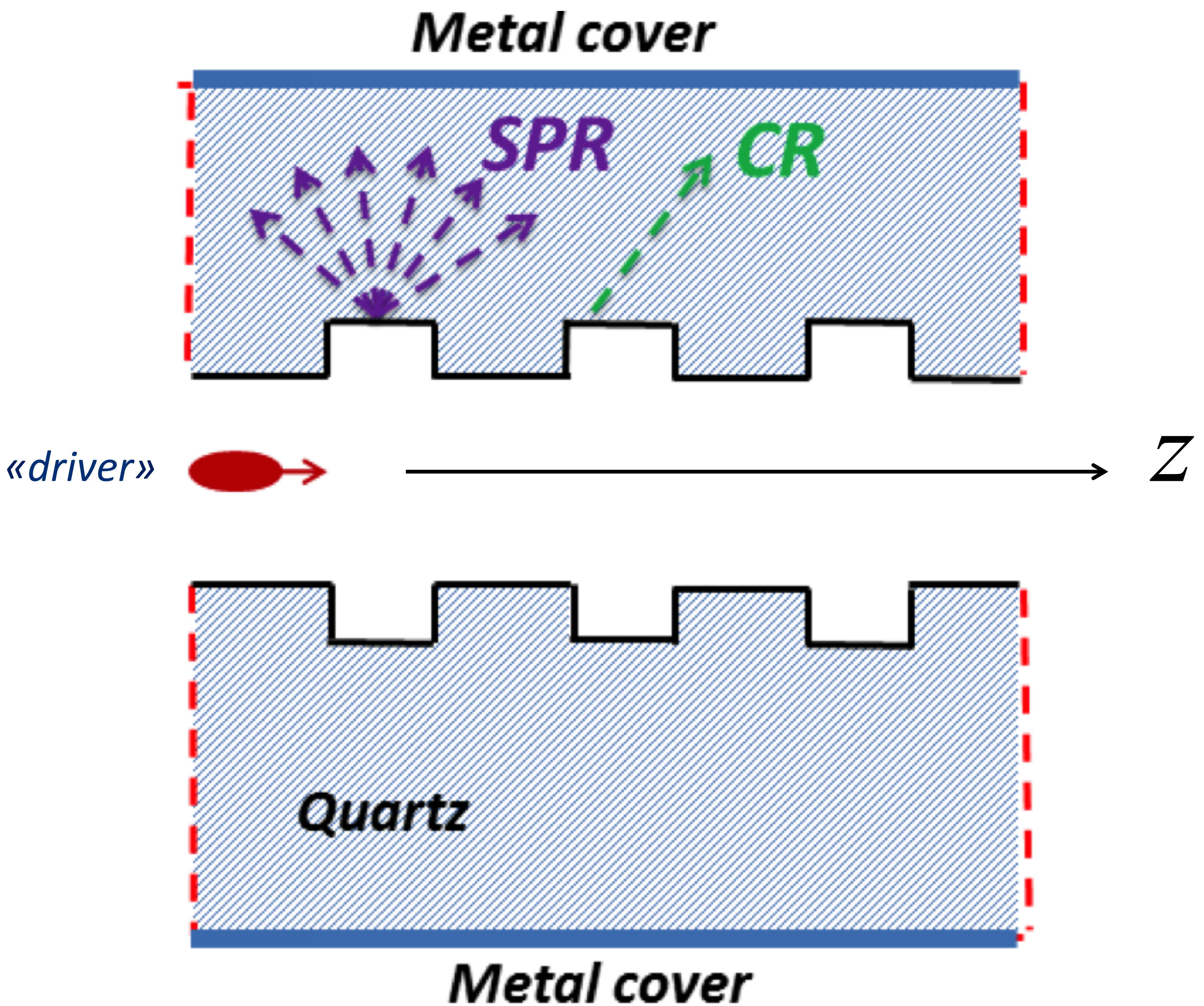

Theoretical result №1 – $E_1(r,\omega)$

A.P. Potylitsyn, M.I. Ryazanov, M.N. Strikhanov, A.A. Tishchenko, Diffraction Radiation from Relativistic Particles, Springer-Verlag, 2010

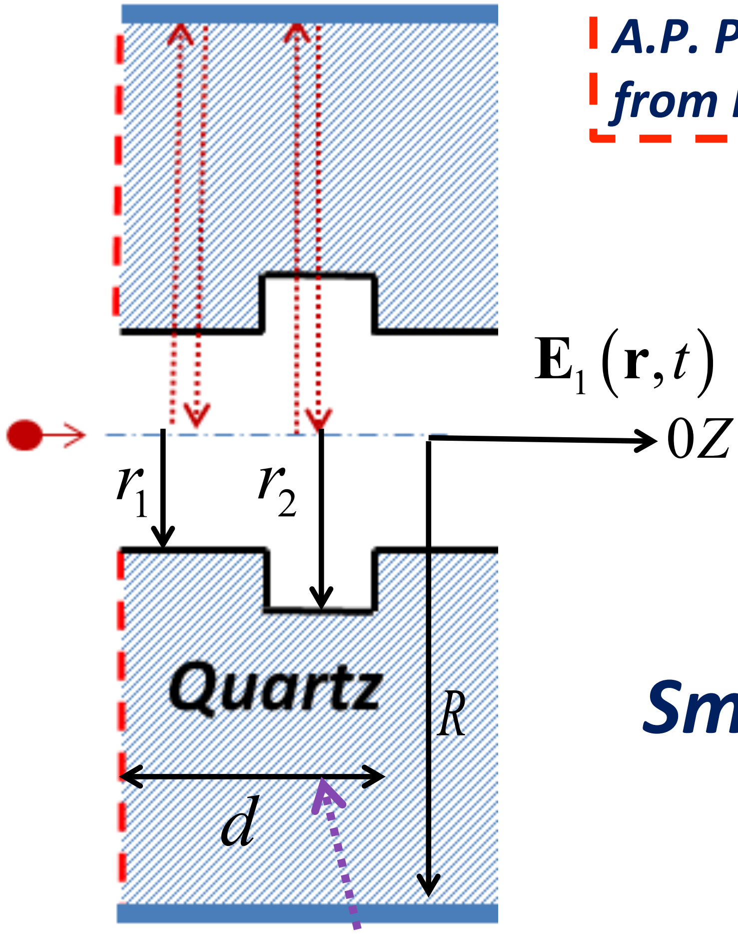

$$\boxed{\mathbf{E}_1(\mathbf{r},t)=\int_{-\infty}^{\infty} d\omega\, e^{-i\omega t}\,\mathbf{E}_1(\mathbf{r},\omega)}$$

$$k=\frac{2\pi}{\lambda}\sqrt{\varepsilon}$$

Smith-Purcell

$$F_1(r)=-k\,r\,J_1(k\,r)K_0\left(\frac{k}{\gamma\beta}r\right)+\frac{k}{\gamma\beta}r\,J_0(k\,r)K_1\left(\frac{k}{\gamma\beta}r\right)$$

$$F_2(r)=k\,r\,J_0(k\,r)K_1\left(\frac{k}{\gamma\beta}r\right)+\frac{k}{\gamma\beta\sqrt{\varepsilon}}r\,J_1(k\,r)K_0\left(\frac{k}{\gamma\beta}r\right)$$

$$\mathbf{E}_1(\mathbf{r},\omega)=i\frac{e(2\pi)^3}{\beta^{-1}}\boxed{\frac{1-e^{-ik\beta^{-1}d\,N}}{1-e^{ik\beta^{-1}d}}}\times$$

$$\times\,\underline{\mathbf{e}_z}\left(\left(e^{-ik\beta^{-1}l}-1\right)\underline{\left(F_1(r_1)-F_1(R)\right)}+\left(e^{-ik\beta^{-1}d}-e^{-ik\beta^{-1}l}\right)\underline{\left(F_1(r_2)-F_1(R)\right)}\right)\times$$

$$\times\,e^{-ik(R-r_2)}\left(\underline{e^{-ika}\sum_n\theta(z-nd)\theta(-z+nd+l)+\sum_n\theta(z-nd-l)\theta(-z+(n+1)d)}\right)$$

Theoretical result №1 – $E_1(r,t)$

$\lambda = 0.3\ mm$
$l = 1\ mm$
$r_1 = 1\ mm$
$R = 2\ mm$
$d = 2l$
$a = 0.2\ mm$
$N = 10$
$\gamma = 16$

$$\mathbf{E}_1(r,t) = i\frac{e(2\pi)^3}{\beta^{-1}}\mathbf{e}_z \int_{-\infty}^{+\infty} d\omega\, e^{-i\omega t} \sum_{n'} e^{-2\pi i \frac{\omega}{c}\beta^{-1} d\, n'} e^{-2\pi i \frac{\omega}{c}(R-r_2)}$$

$$\times\left(\left(e^{-ik\beta^{-1}l}-1\right)\left(F_1(r_1)-F_1(R)\right)+\left(e^{-ik\beta^{-1}d}-e^{-ik\beta^{-1}l}\right)\left(F_1(r_2)-F_1(R)\right)\right)\times$$

$$\times\left(e^{-ika}\sum_n \theta(z-nd)\theta(-z+nd+l)+\sum_n \theta(z-nd-l)\theta(-z+(n+1)d)\right)$$

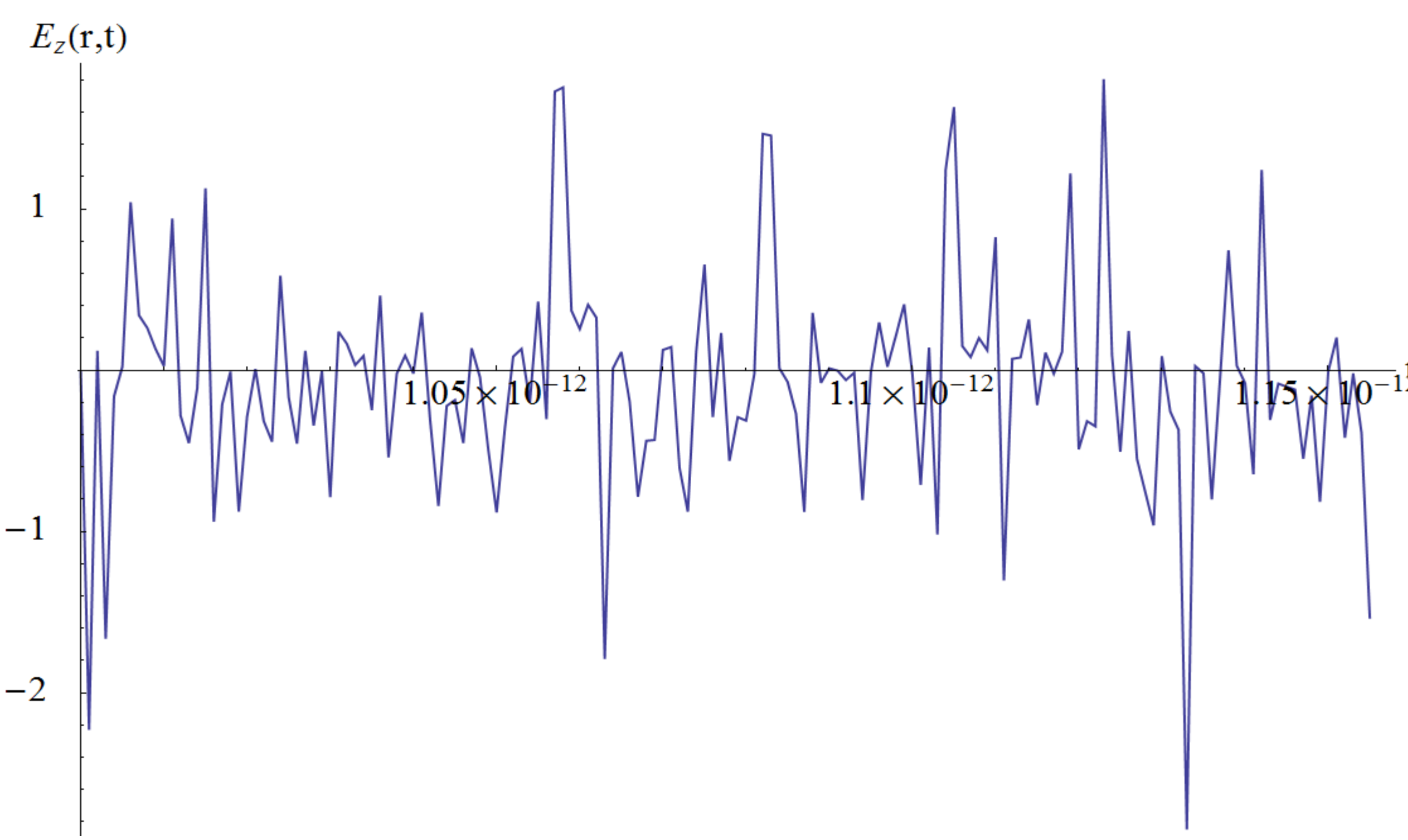

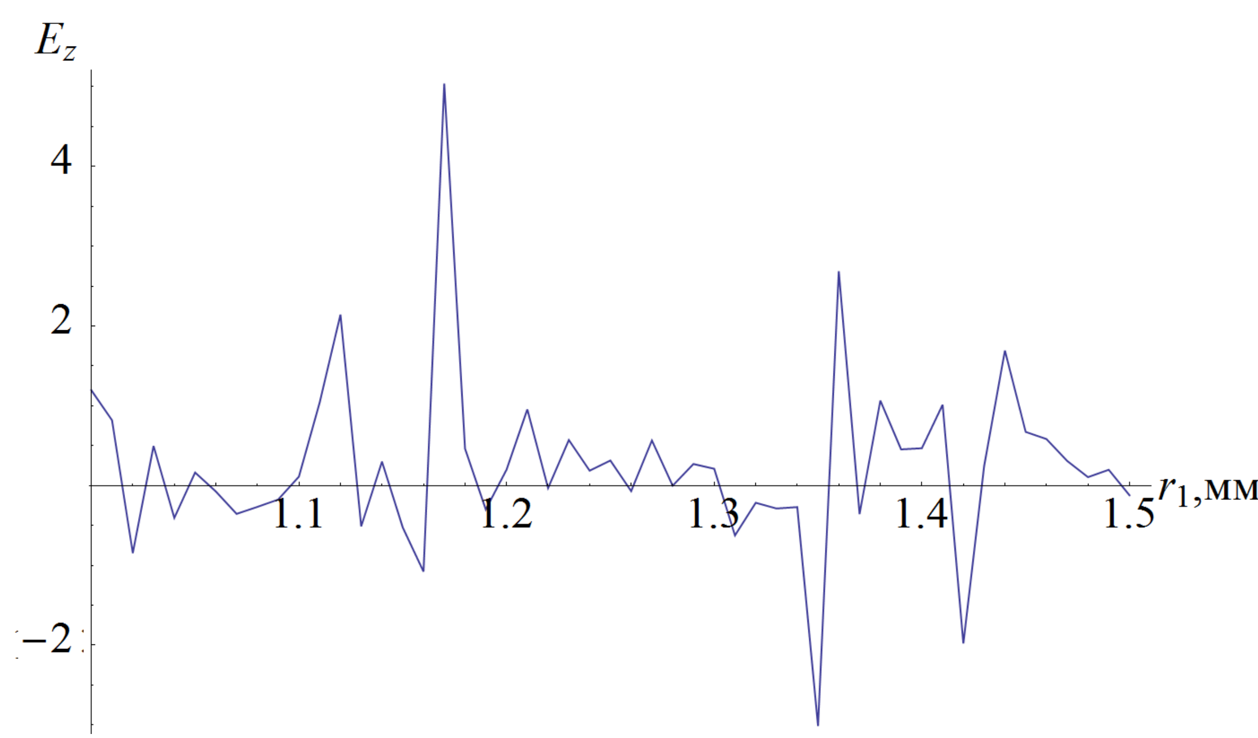

Layout №2 – wakefield acceleration

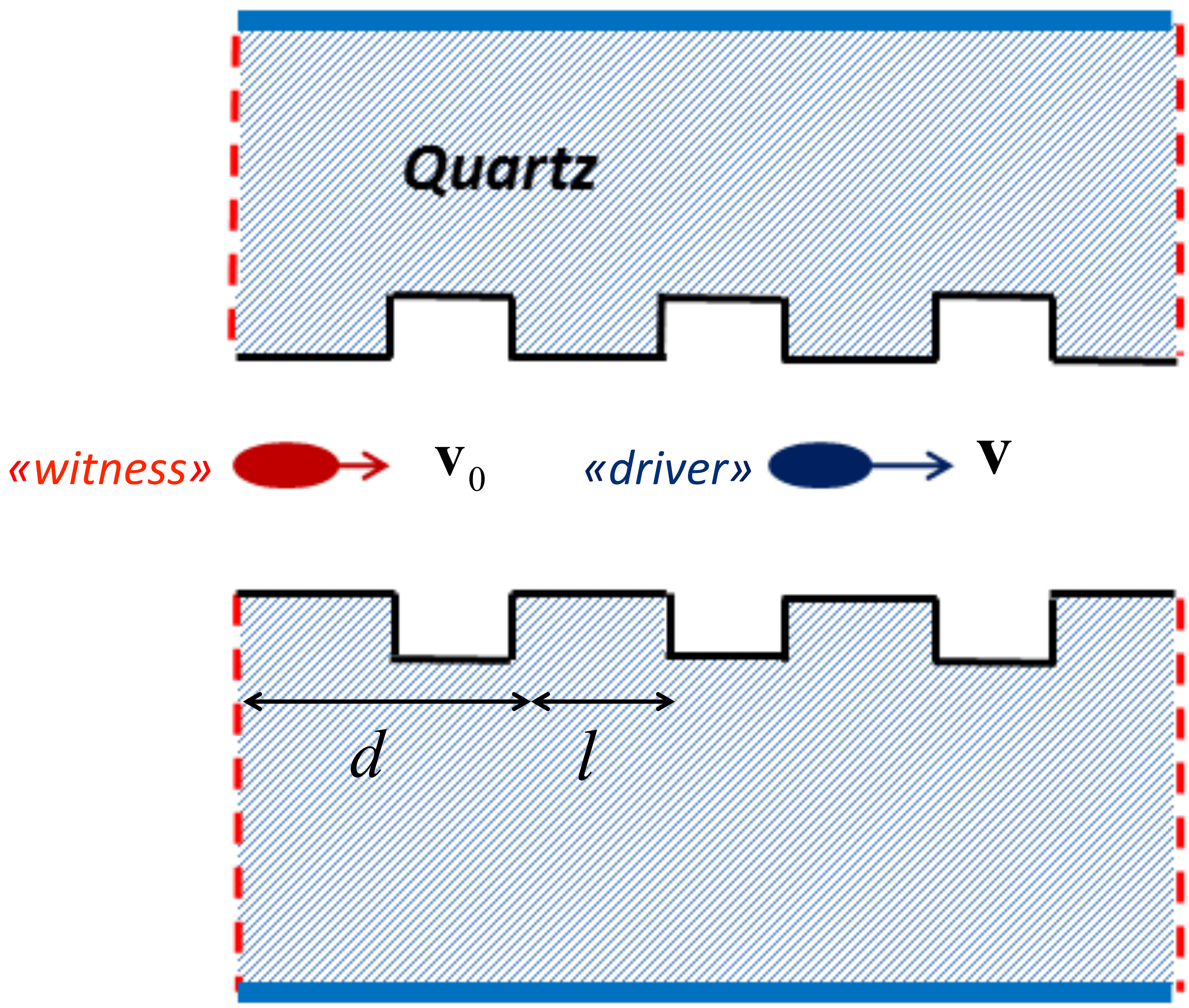

Theoretical result №2 – $E_2(r,t)$

$$\mathbf{E}_2(r,t)=i\frac{e(2\pi)^3}{\beta^{-1}}\mathbf{e}_z\int_{-\infty}^{+\infty}d\omega\, e^{-i\omega t}\sum_{n'}e^{-2\pi i\frac{\omega}{c}\beta^{-1}d\,n'}\,e^{-2\pi i\frac{\omega}{c}(R-r_2)}\times$$
$$\times\left(\left(e^{-ik\beta^{-1}l}-1\right)\left(F_1(r_1)-F_1(R)\right)+\left(e^{-ik\beta^{-1}d}-e^{-ik\beta^{-1}l}\right)\left(F_1(r_2)-F_1(R)\right)\right)\times$$
$$\times\left(e^{-ika}\,\theta(v_0t)\,\theta(-v_0t+l)+\theta(v_0t-l)\,\theta(-v_0t+2d)\right)$$

$\lambda=0.3\ mm$

$l=1\ mm$

$r_1=1\ mm$

$R=2\ mm$

$d=2l$

$a=0.2\ mm$

$N=10$

$\gamma=16$

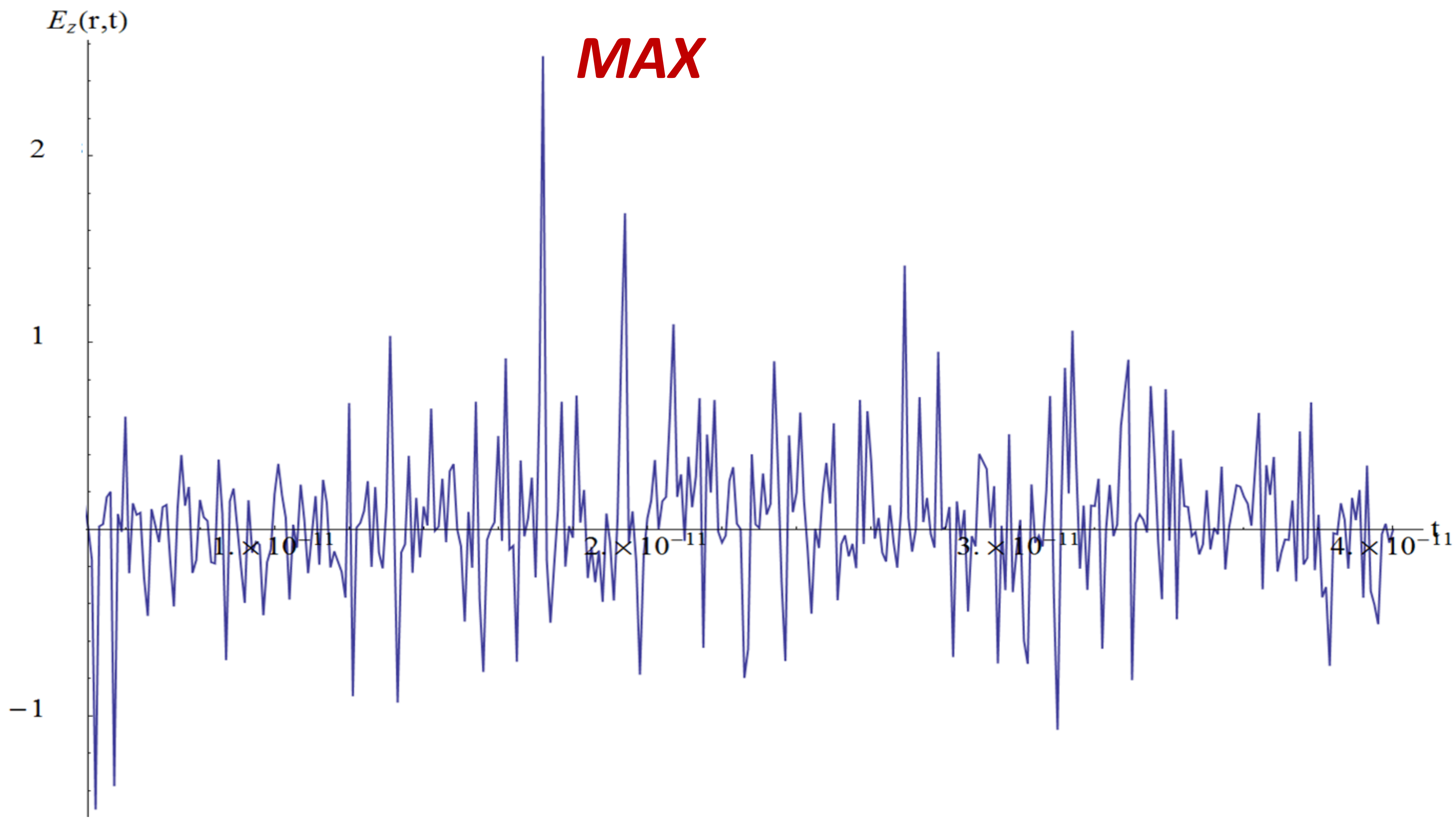

VSim simulations

- 3D simulations of the electric field in corrugated and flat capillary were performed in VSim (VORPAL physics engine).
- **Electron beam was simulated as a Gaussian charge density distribution** on-axis, no macro-particles in the calculation domain.
- **Dielectric losses** were not taken into account.

Longitudinal electric field Ez in Oyz cross-section:

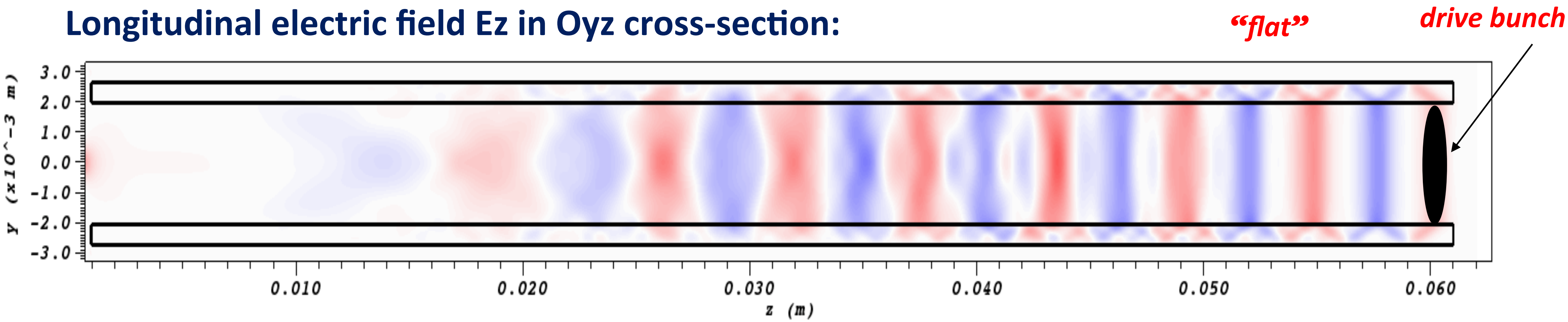

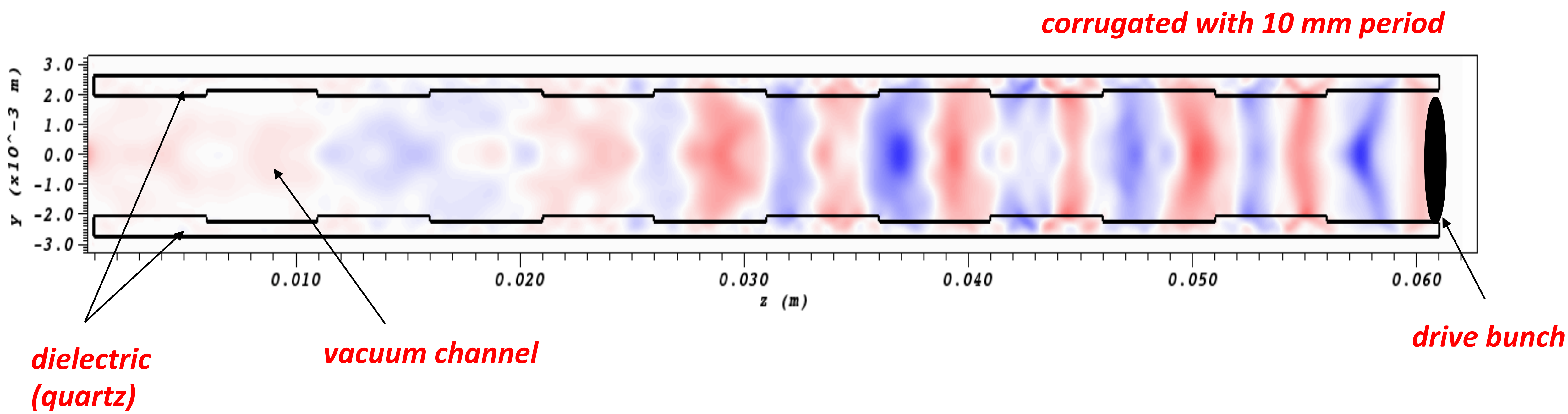

VSim simulations. Single drive case.

LUCX beam parameters:

No of drives	Charge	σ_z
1	100 pC	0.3 mm
2	33; 100 pC	0.2; 0.3 mm
3	33; 66; 100 pC	0.2; 0.25; 0.3 mm
4	25; 50; 75; 100 pC	0.2; 0.233; 0.266; 0.3 mm

On-axis longitudinal field in flat and corrugated capillary with 10 mm period

Shift of main accelerating mode **from 50 GHz to 55 GHz** in corrugated capillary with 10 mm period

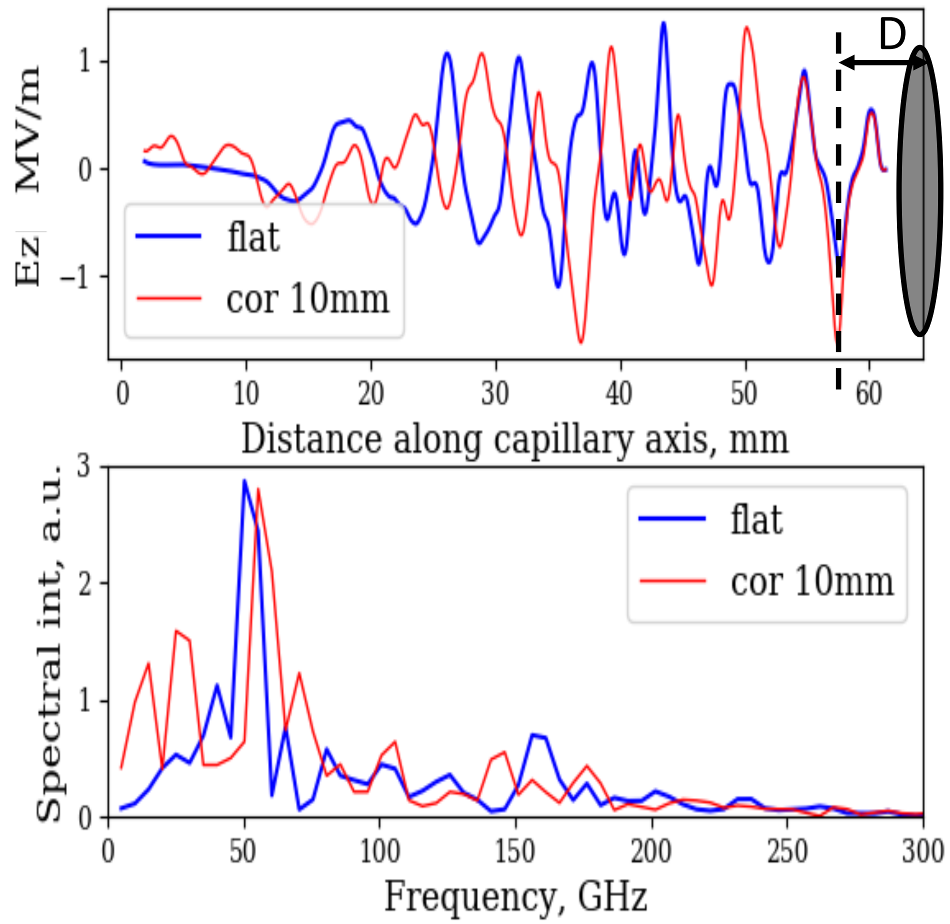

drive

D – distance from the drive to the first accelerating peak

K.Lekomtcev et al., Driver-witness electron beam acceleration in dielectric mm-scale capillaries, PHYSICAL REVIEW ACCELERATORS AND BEAMS 21, 051301 (2018)

VSim simulations for 1-st acceleration peak

Electric field at first accelerating peak as a function of distance along capillary

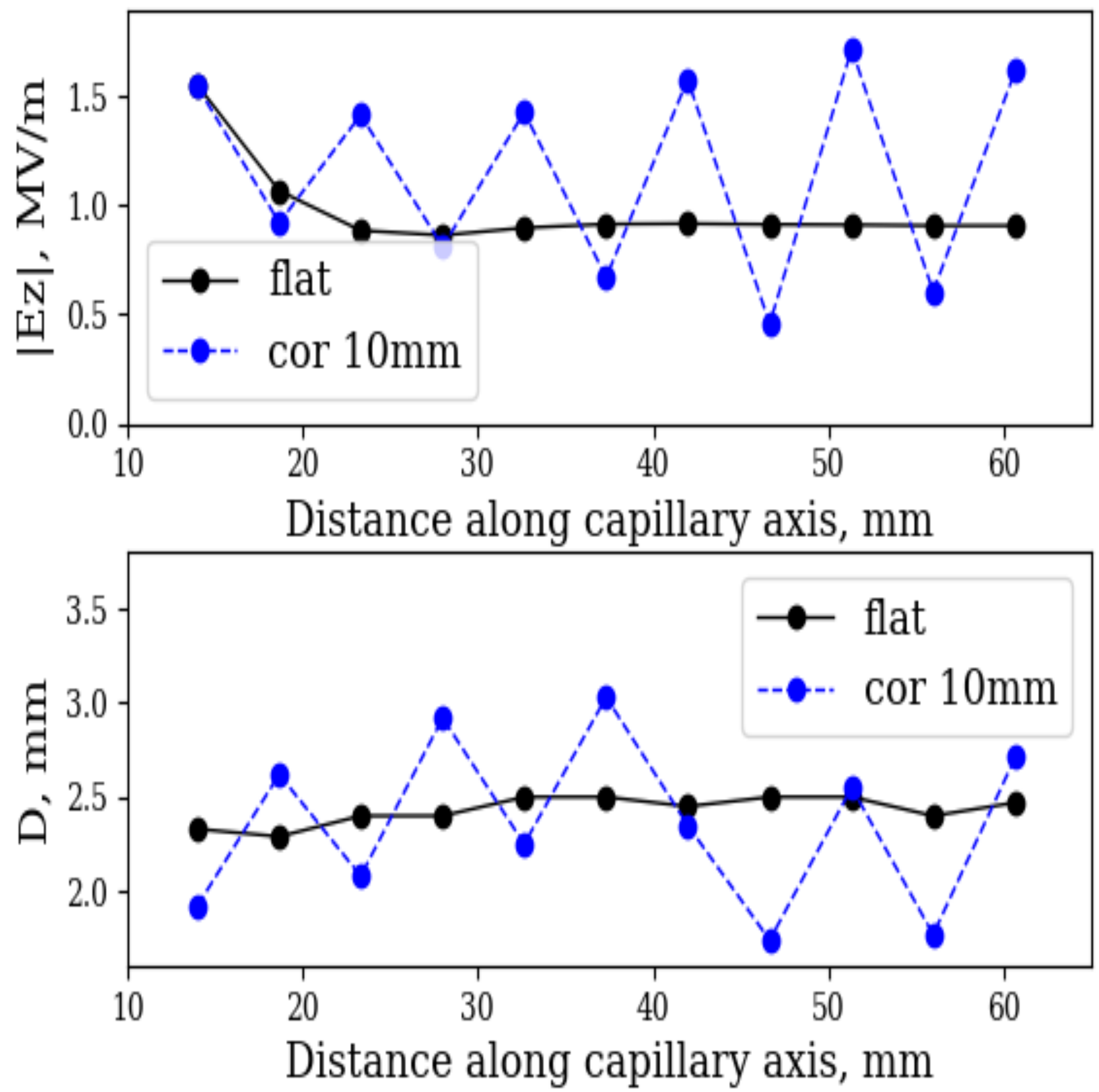

Distance D as function of distance along capillary

Average accelerating field along capillary as a function of corrugation period

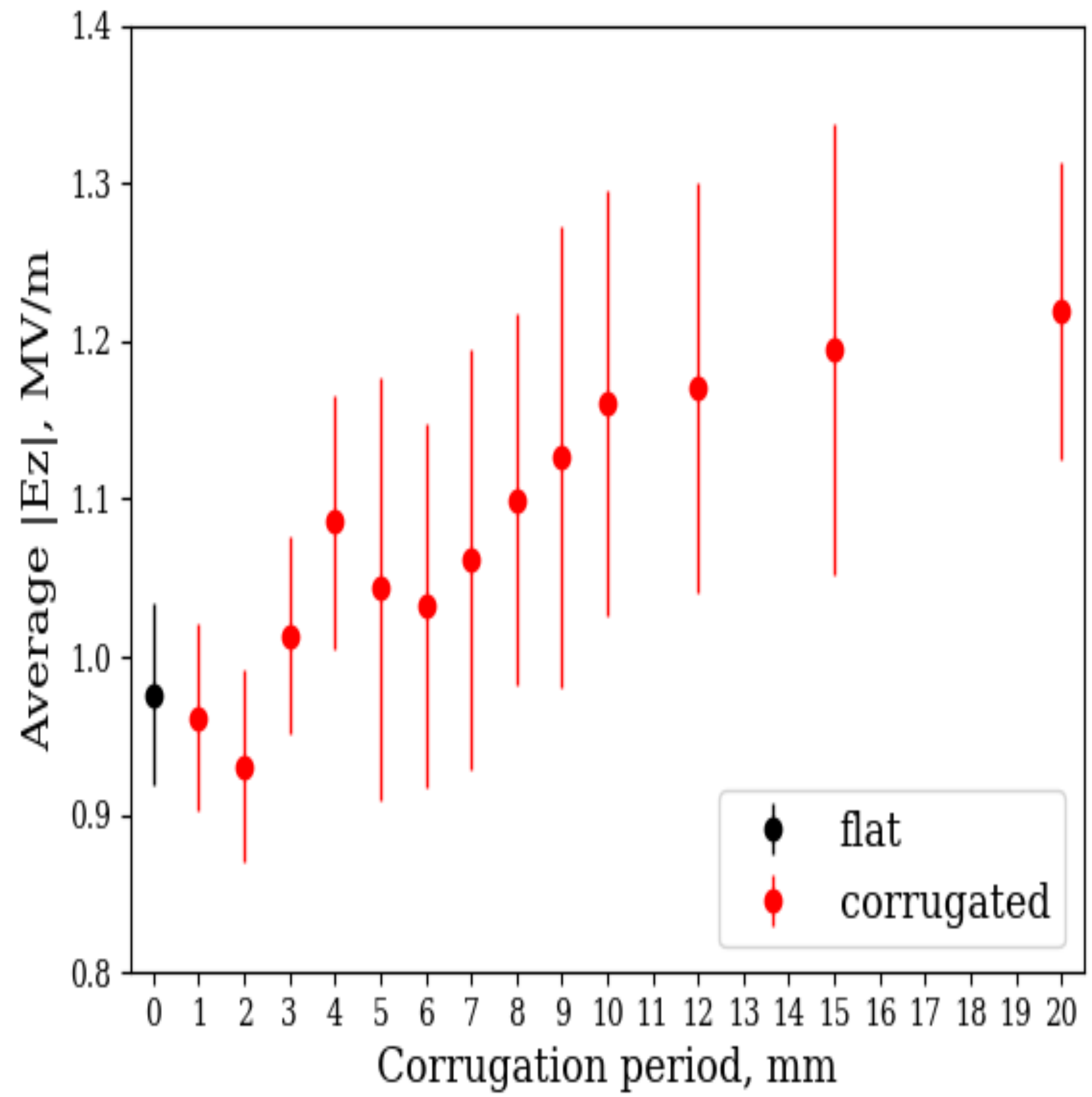

VSim simulations. Multi-drive case.

- Simulations were performed for **equidistant** bunch trains.
- 2^{nd}, 3^{rd} and 4^{th} bunches were positioned at accelerating phases of on-axis longitudinal field.
- Bunch separation was **5.8 mm** for flat and **5.4 mm** for corrugated capillary with **10 mm** period.

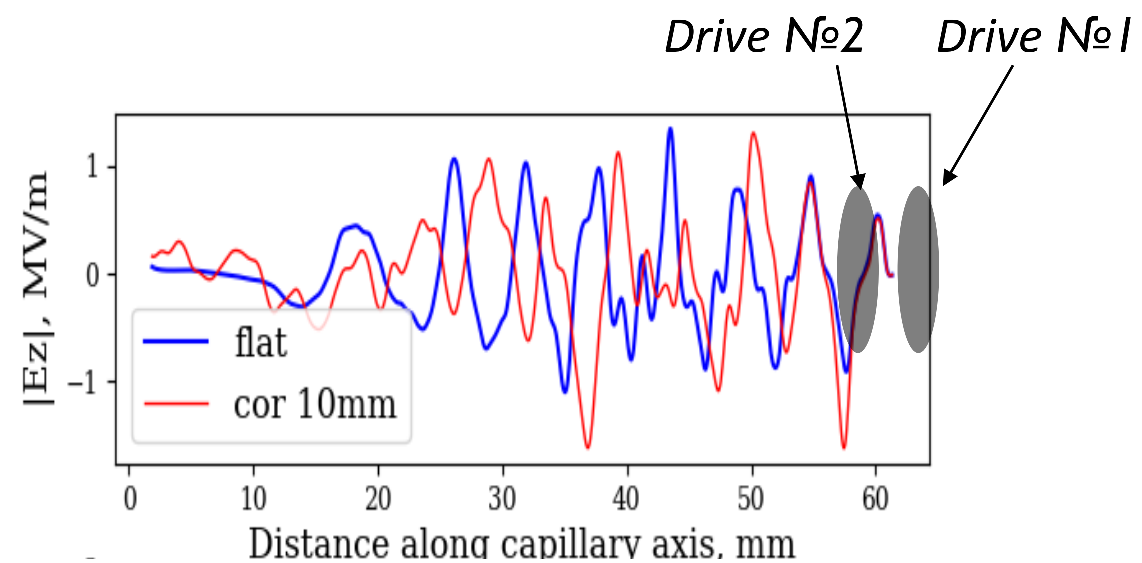

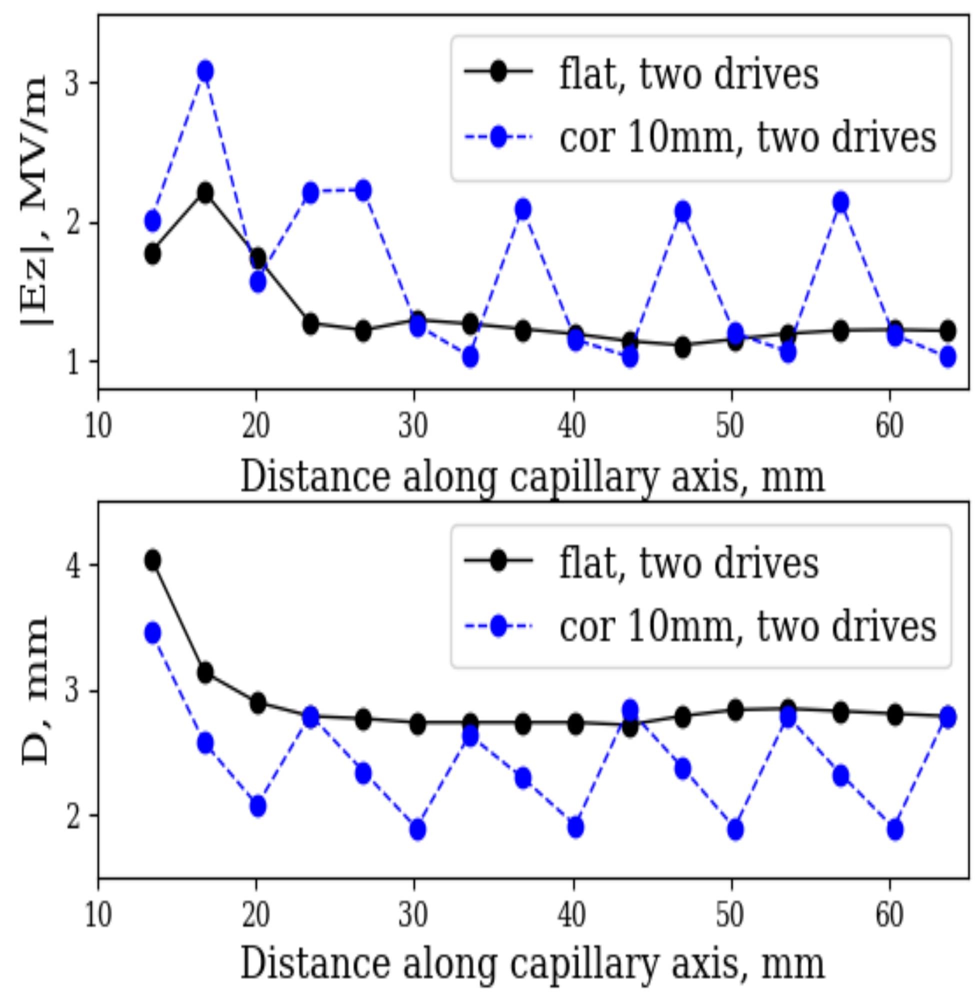

Summary and plans

- *For a **single drive** simulation showed **18.9% increase** in the accelerating field for the corrugation period 10mm with **stability of the first accelerating peak 2.36±0.13 mm**, in terms of distance to the preceding drive bunch*

- *For a ramped **two-drive train** simulations showed **22.9%** increase in the accelerating field for the corrugation period 10mm with stability of the first accelerating peak of **2.43±0.11 mm***

- *Two drives have stabilizing effect on the phase of the accelerating field. As shown the RMS errors of the **phase stability reduced** from 0.13 mm (1 drive) to 0.11 mm (2 drives)*

- ***Higher relative increase of the accelerating field can be achieved by using larger corrugation period and bunch trains with variable bunch-to-bunch separation***

- ***Comparison between simulation and theory***

Thank you for your attention!

Capillary with periodic radius

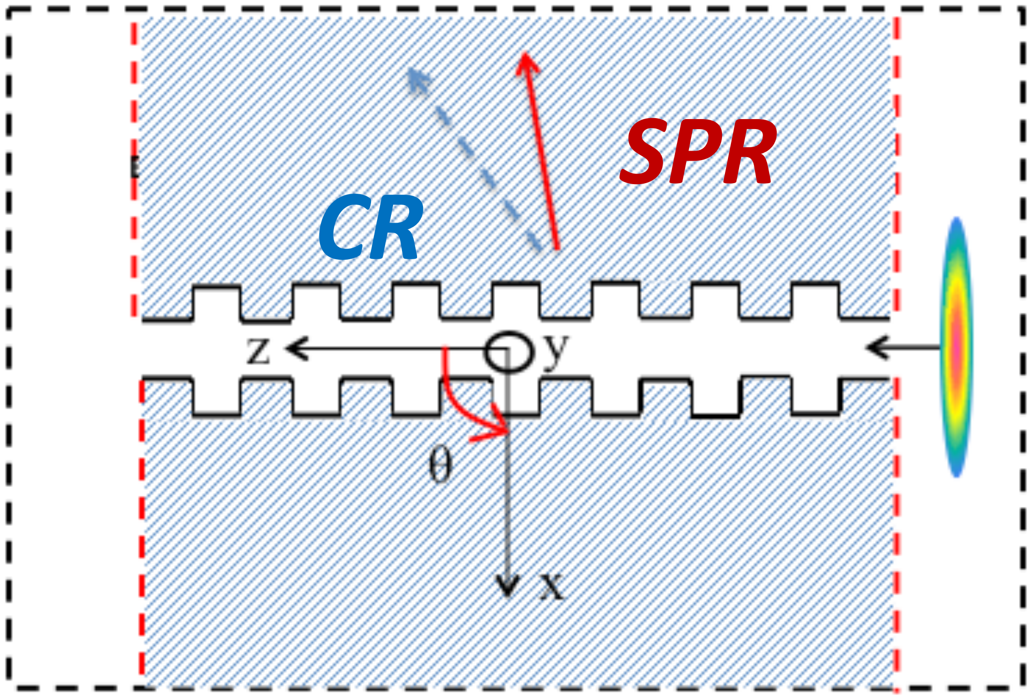

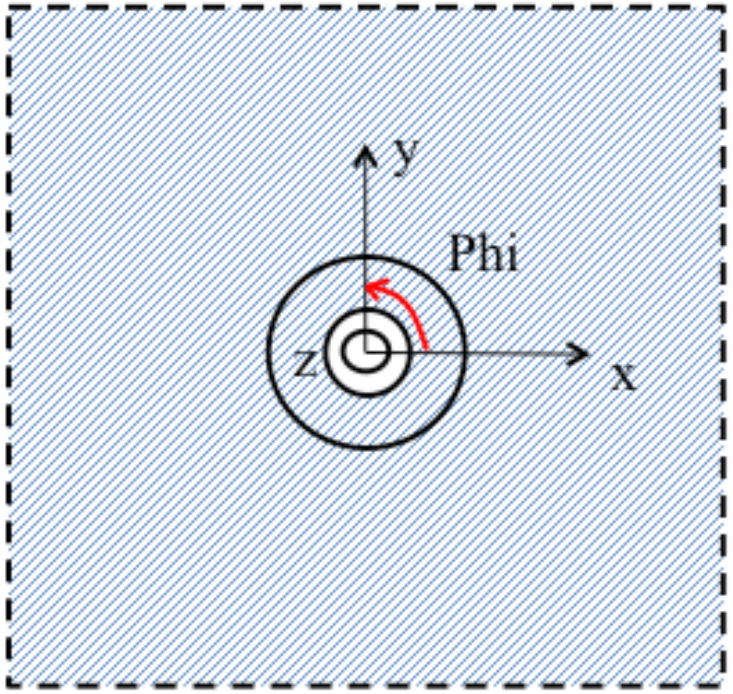

SPR as source of powerful THz radiation – SPR > CR!

A.A. Ponomarenko, M.I. Ryazanov, M.N. Strikhanov, A.A. Tishchenko, Terahertz Radiation from Electrons Moving through a Waveguide with Variable Radius, based on Smith-Purcell and Cherenkov Mechanisms, Nucl. Instr. and Meth. B 309, 223-225 (2013).

A.A. Ponomarenko, K.V. Lekomtsev, A.A. Tishchenko, M.N. Strikhanov, J. Urakawa, CST simulation of THz radiation from a channel with periodically variable radius, Nucl. Instr. and Meth. B 355, 160-163 (2015).

A.A. Ponomarenko, M.I. Ryazanov, M.N. Strikhanov, A.A. Tishchenko, Terahertz Radiation from Electrons Moving through a Waveguide with Variable Radius, based on Smith-Purcell and Cherenkov Mechanisms, Nucl. Instr. and Meth. B 309, 223-225 (2013).

A.A. Ponomarenko, K.V. Lekomtsev, A.A. Tishchenko, M.N. Strikhanov, J. Urakawa, CST simulation of THz radiation from a channel with periodically variable radius, Nucl. Instr. and Meth. B 355, 160-163 (2015).

Experiment №1 – LUCX, KEK, Japan

Sub-THz radiation from dielectric capillaries with reflectors

K. Lekomtsev [a,*], A. Aryshev [b], A.A. Tishchenko [c], M. Shevelev [b], A.A. Ponomarenko [c], P. Karataev [a], N. Terunuma [b,d], J. Urakawa [b]

[a] *John Adams Institute at Royal Holloway University of London, Egham, Surrey TW20 0EX, UK*
[b] *KEK: High Energy Accelerator Research Organization, 1-1 Oho, Tsukuba, Ibaraki 305-0801, Japan*
[c] *National Research Nuclear University MEPhI, Kashirskoe sh. 31, Moscow 116409, Russia*
[d] *SOKENDAI: The Graduate University for Advanced Studies, 1-1 Oho, Tsukuba, Ibaraki 305-0801, Japan*

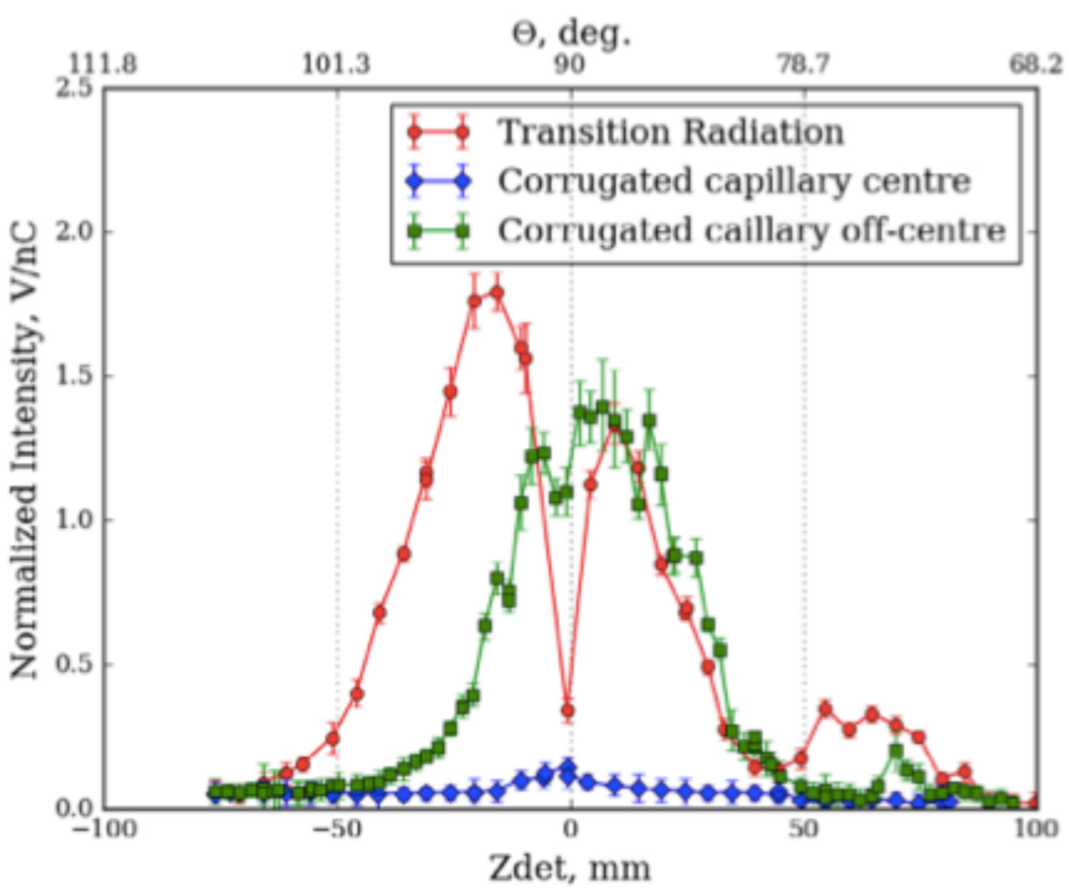

Fig. 2. Crosscheck with Transition Radiation.

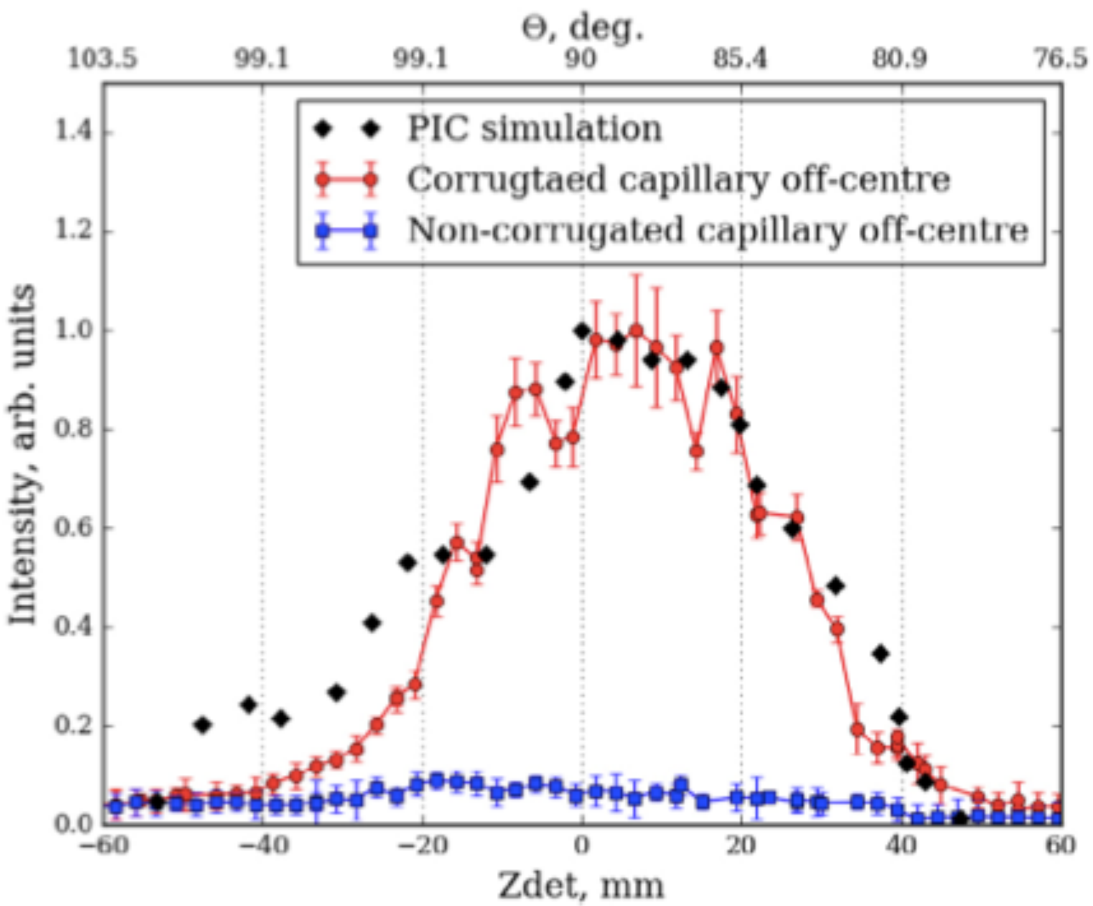

Fig. 3. Radiation distribution along axis z. (For interpretation of the references to colour in this figure legend, the reader is referred to the web version of this article.)

Discussions and plans

- **Some preliminary theoretical results for accelerator field**

Nearest plans:

- **Comparison with computer simulation (CST)**
- **More detailed investigation of accelerated motion**

Driver-witness electron beam acceleration in dielectric mm-scale capillaries

K. Lekomtsev,[1,*] A. Aryshev,[2,3] A. A. Tishchenko,[4,5] M. Shevelev,[6] A. Lyapin,[1] S. Boogert,[1]
P. Karataev,[1] N. Terunuma,[2,3] and J. Urakawa[2]

[1]*John Adams Institute at Royal Holloway, University of London, Egham, Surrey TW20 0EX, United Kingdom*
[2]*KEK: High Energy Accelerator Research Organization, 1-1 Oho, Tsukuba, Ibaraki 305-0801, Japan*
[3]*SOKENDAI: The Graduate University for Advanced Studies, 1-1 Oho, Tsukuba, Ibaraki 305-0801, Japan*
[4]*National Research Nuclear University MEPhI, Kashirskoe Highway, 31, Moscow 115409, Russian Federation*
[5]*National Research Center Kurchatov Institute, Akademika Kurchatova pl. 1, Moscow 123182, Russian Federation*
[6]*Tomsk Polytechnic University, Institute of Physics and Technology, Lenin Avenue 30, Tomsk 634050, Russian Federation*

- **MultiGeV/m gradients** (charging the dielectric surface by halo vs space charge effect, longitudinal modes)

Non-central propagation

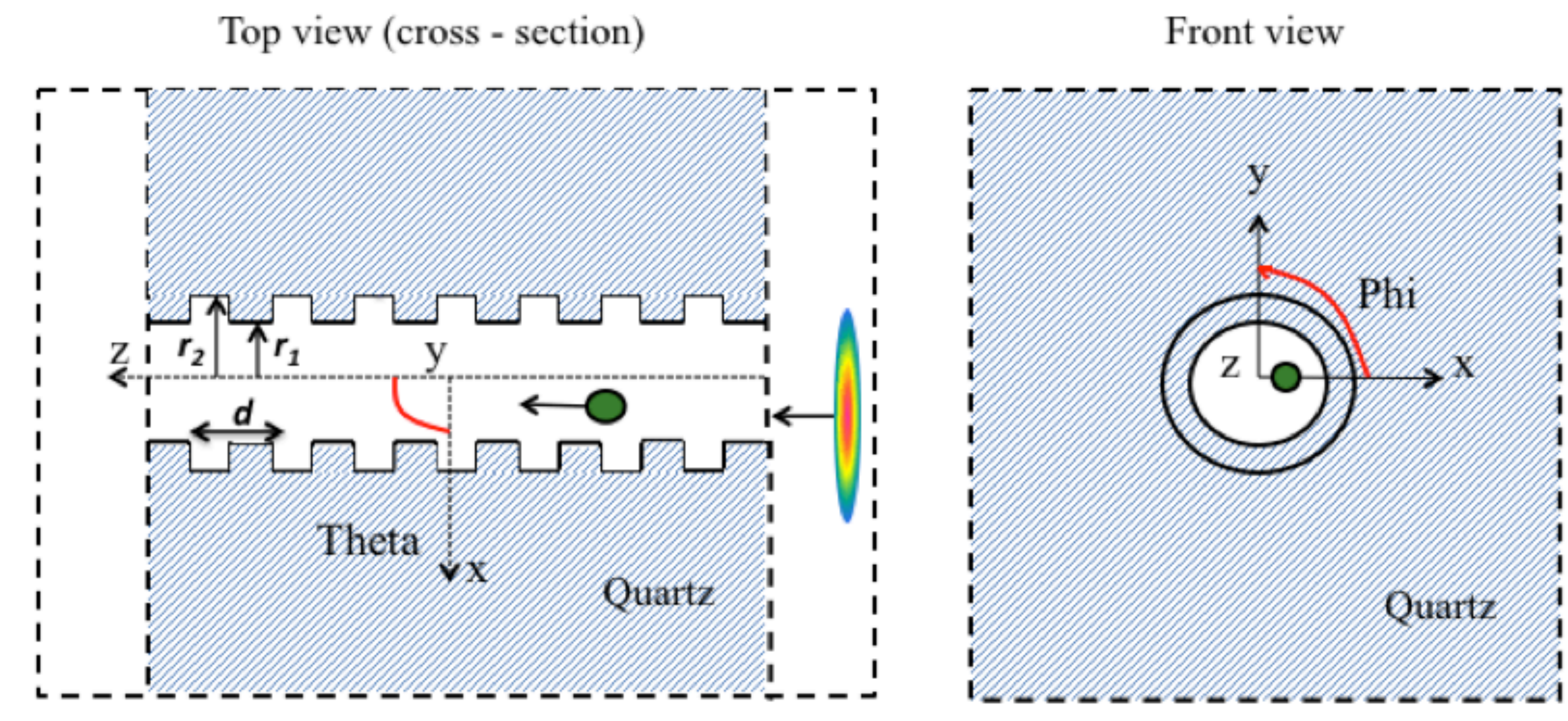

$$b << r$$

A.A. Ponomarenko, A.A. Tishchenko, M.N. Strikhanov, THz polarization radiation from electrons passing corrugated dielectric tube under non-central propagation, Nucl. Instr. and Meth. B 400 (2017)

Theoretical background - analysis

$$\frac{d^2W}{d\Omega\, d\hbar\omega}=\frac{4\,e^2\gamma^2(\varepsilon-1)^2}{(2\pi)^2 c\sqrt{\varepsilon}\left(1+\gamma^2\beta^2\varepsilon\sin^2\theta\right)^2}\times\frac{\sin^2\left(\frac{1}{2}k\varphi\, d\, N\right)}{\sin^2\left(\frac{1}{2}k\varphi\, d\right)}\times\left(N_e+(N_e-1)\frac{1}{\pi^2}e^{-\frac{k^2}{2}\left(r_b^2+\left(\beta\sqrt{\varepsilon}\right)^{-1}\frac{l_b^2}{4}\right)}\right)\times$$

$$\times\frac{\left|\cos\theta\,\gamma^{-1}\left(\left(e^{-ik\varphi l}-1\right)F_1(r_1)+\left(e^{-ik\varphi d}-e^{-ik\varphi l}\right)F_1(r_2)\right)+\sin\theta\left(\left(e^{-ik\varphi l}-1\right)F_2(r_1)+\left(e^{-ik\varphi d}-e^{-ik\varphi l}\right)F_2(r_2)\right)\right|^2}{\left(\cos\theta-\left(\beta\sqrt{\varepsilon}\right)^{-1}\right)^2}$$

$$\frac{\sin^2\left(\frac{k}{2}\left(\cos\theta-\left(\beta\sqrt{\varepsilon}\right)^{-1}\right)d\,N\right)}{\sin^2\left(\frac{k}{2}\left(\cos\theta-\left(\beta\sqrt{\varepsilon}\right)^{-1}\right)d\right)}\Rightarrow\frac{d}{\lambda}\left(-\sqrt{\varepsilon}+1\right)\le n\le\frac{d}{\lambda}\left(\sqrt{\varepsilon}+1\right)$$

$$F_1(r)=-kr\cos\theta\,J_1(kr\cos\theta)K_0\left(\frac{k}{\gamma\beta\sqrt{\varepsilon}}r\right)+\frac{k}{\gamma\beta\sqrt{\varepsilon}}r\,J_0(kr\cos\theta)K_1\left(\frac{k}{\gamma\beta\sqrt{\varepsilon}}r\right)$$

$$F_2(r)=kr\cos\theta\,J_0(kr\cos\theta)K_1\left(\frac{k}{\gamma\beta\sqrt{\varepsilon}}r\right)+\frac{k}{\gamma\beta\sqrt{\varepsilon}}r\,J_1(kr\cos\theta)K_0\left(\frac{k}{\gamma\beta\sqrt{\varepsilon}}r\right)$$

$$\varphi=\cos\theta-\left(\beta\sqrt{\varepsilon}\right)^{-1}$$

$$\cos\theta=\left(\beta\sqrt{\varepsilon}\right)^{-1}$$

A.A. Ponomarenko, M.I. Ryazanov, M.N. Strikhanov, A.A. Tishchenko, Terahertz Radiation from Electrons Moving through a Waveguide with Variable Radius, based on Smith-Purcell and Cherenkov Mechanisms, Nucl. Instr. and Meth. B 309, 223-225 (2013).

$$\frac{d^2W}{d\Omega\, d\hbar\omega} = \frac{d^2W_0}{d\Omega\, d\hbar\omega} + \frac{1}{137}\frac{\gamma^2(\varepsilon-1)^2}{(2\pi)^2\sqrt{\varepsilon}}\frac{\sin^2\left(\frac{1}{2}k\,\tilde{\varphi}\,d\,N\right)}{\sin^2\left(\frac{1}{2}k\,\tilde{\varphi}\,d\right)}\frac{\sin\left(k\,\tilde{\varphi}(d-l)\right)+\sin\left(k\,\tilde{\varphi}\,l\right)-\sin\left(k\,\tilde{\varphi}\,d\right)}{\tilde{\varphi}^2}\times$$
$$\times 2b\left\{\left(\sin\theta\, F_{12}+\cos\theta\, F_{22}\right)\left(\chi_1+\eta_1\right)-\left(\sin\theta\, F_{11}+\cos\theta\, F_{21}\right)\left(\chi_2+\eta_2\right)\right\}$$

$$\chi_i(r_i,R)=\left(\frac{k}{\beta\gamma\sqrt{\varepsilon}}\right)^2\cos\theta\cos\varphi'\left(1+\gamma^2\beta^2\varepsilon\sin^2\theta\right)\int_{r_i}^{R}dr\, r\left(\cos^2\varphi'\, J_0(kr\sin\theta)-\frac{\cos 2\varphi'}{kr\sin\theta}J_1(kr\sin\theta)\right)\times$$
$$\times\left(\frac{k}{2\beta\gamma\sqrt{\varepsilon}}\left(K_0\left(\frac{k}{\beta\gamma\sqrt{\varepsilon}}r\right)+K_2\left(\frac{k}{\beta\gamma\sqrt{\varepsilon}}r\right)\right)-\frac{K_1\left(\frac{k}{\beta\gamma\sqrt{\varepsilon}}r\right)}{r}\right)+\frac{J_0(kr\sin\theta)K_1\left(\frac{k}{\beta\gamma\sqrt{\varepsilon}}\delta r\right)}{r}$$

$$\tilde{\varphi}=\cos\theta-\left(\beta\sqrt{\varepsilon}\right)^{-1}$$

$$\eta_i(r_i,R)=\left(\frac{k}{\beta\gamma\sqrt{\varepsilon}}\right)^3\frac{\gamma^{-1}}{2}\sin\theta\cos\varphi'\left(1+\gamma^2\beta^2\varepsilon\sin^2\theta\right)\int_{r_i}^{R}dr\, r\, J_1(kr\sin\theta)\, K_1\left(\frac{k\,r}{\beta\gamma\sqrt{\varepsilon}}\right)$$

$$F_{1i}(r)=-kr_i\sin\theta\, J_1(kr_i\sin\theta)K_0\left(\frac{k}{\gamma\beta\sqrt{\varepsilon}}r_i\right)+\frac{k}{\gamma\beta\sqrt{\varepsilon}}r_i\, J_0(kr_i\sin\theta)K_1\left(\frac{k}{\gamma\beta\sqrt{\varepsilon}}r_i\right)$$

$$F_{2i}(r)=kr_i\sin\theta\, J_0(kr_i\sin\theta)K_1\left(\frac{k}{\gamma\beta\sqrt{\varepsilon}}r_i\right)+\frac{k}{\gamma\beta\sqrt{\varepsilon}}r_i\, J_1(kr_i\sin\theta)K_0\left(\frac{k}{\gamma\beta\sqrt{\varepsilon}}r_i\right)$$

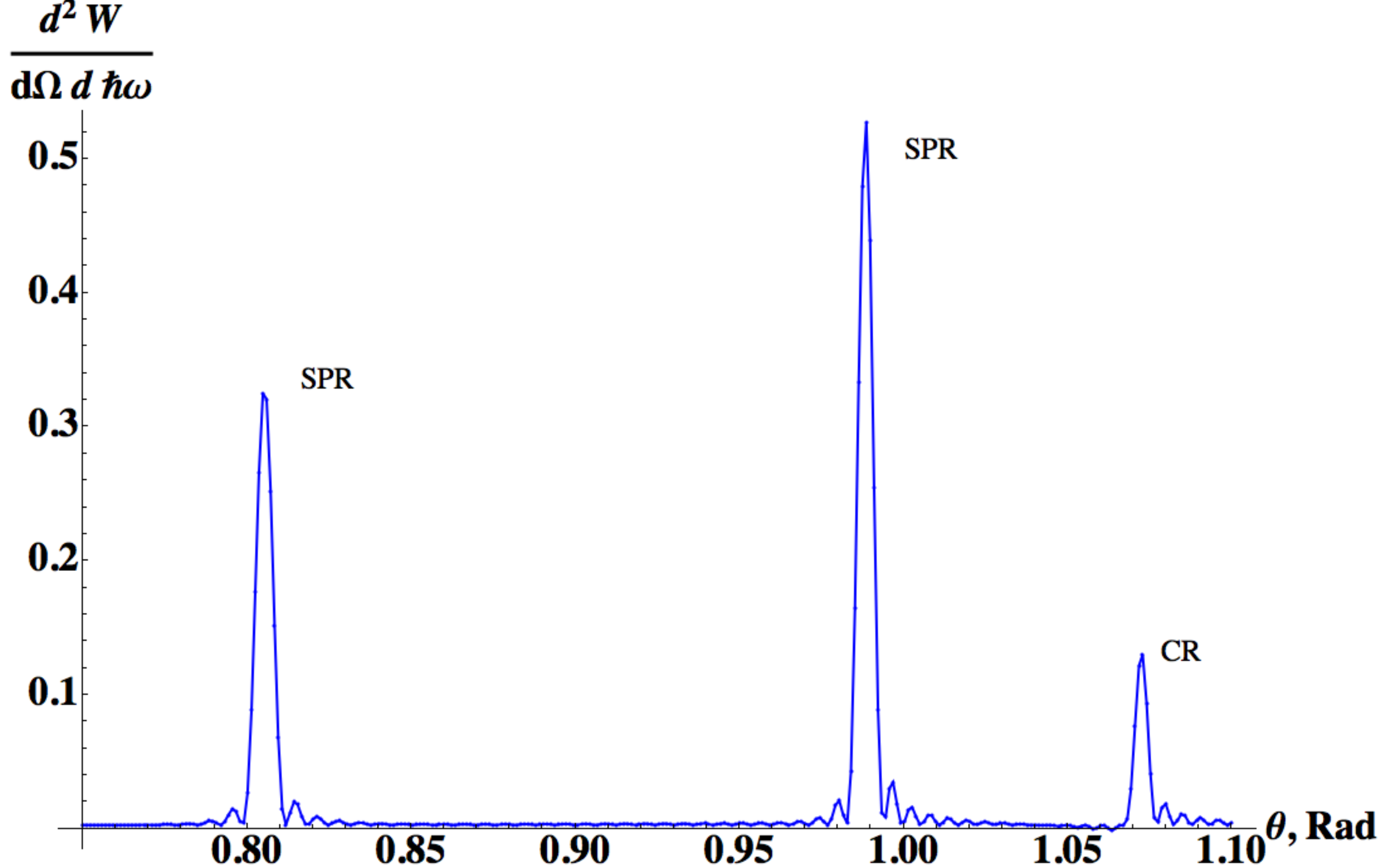

$$\lambda = 0.3\ mm$$
$$N = 15$$
$$d = 2l = 2\ mm$$
$$\gamma = 10$$
$$r_1 = 0.3\ mm$$
$$r_2 = 0.9\ mm$$
$$b = 0.1\ mm$$

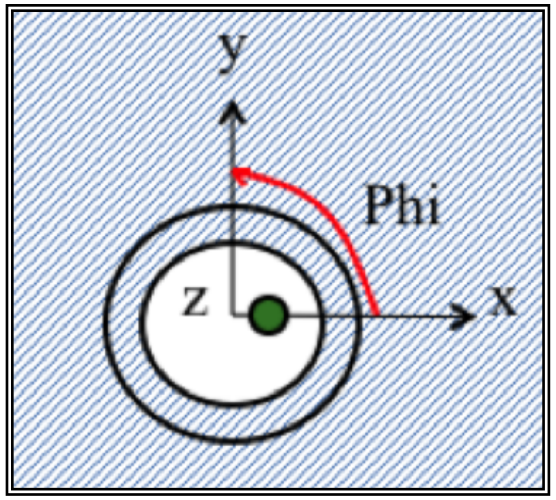

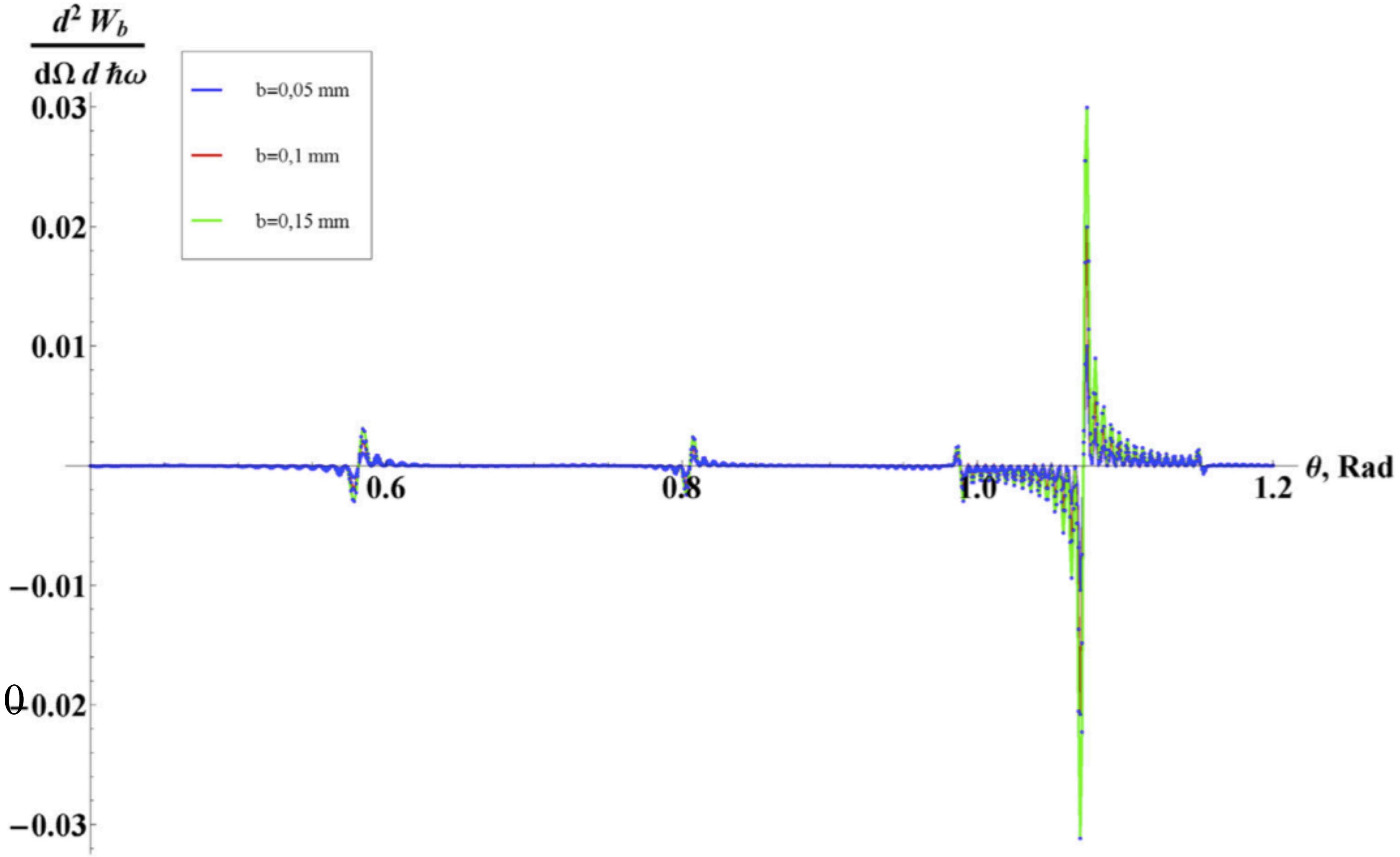

SPR – "b"

CR – "b^2"

$$\frac{\sin\left(k\,\tilde{\varphi}\left(d-l\right)\right)+\sin\left(k\,\tilde{\varphi}\,l\right)-\sin\left(k\,\tilde{\varphi}\,d\right)}{\tilde{\varphi}^2}\xrightarrow{\tilde{\varphi}\to 0} 0$$

$$\tilde{\varphi} = \cos\theta - \left(\beta\sqrt{\varepsilon}\right)^{-1}$$

Theoretical background - analysis

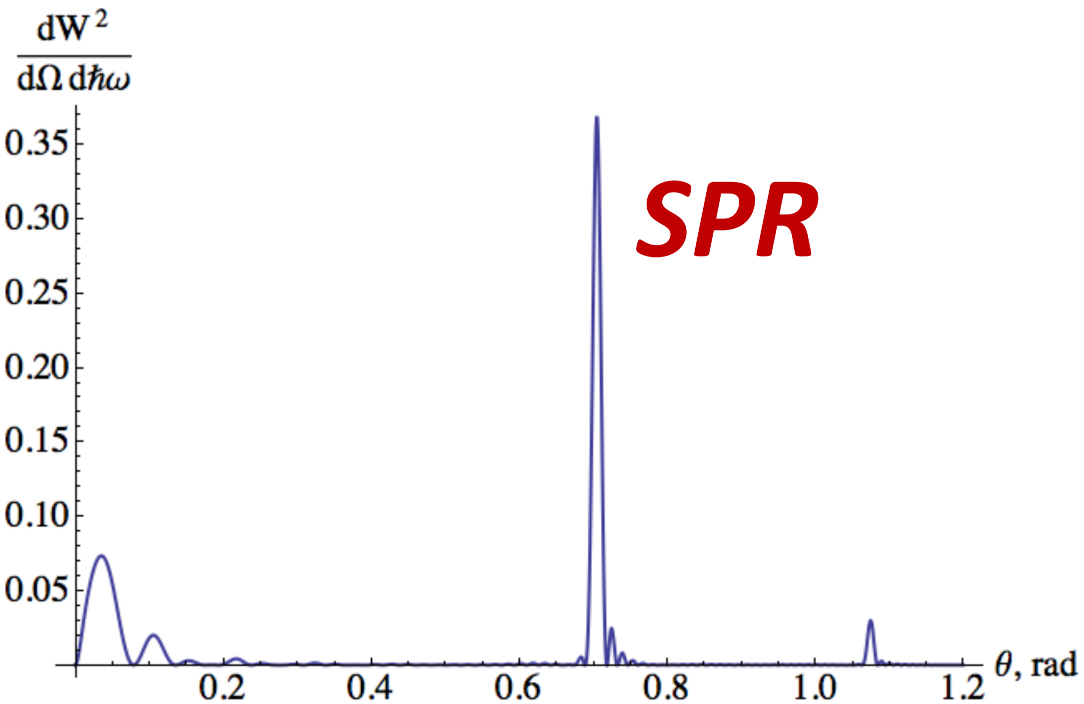

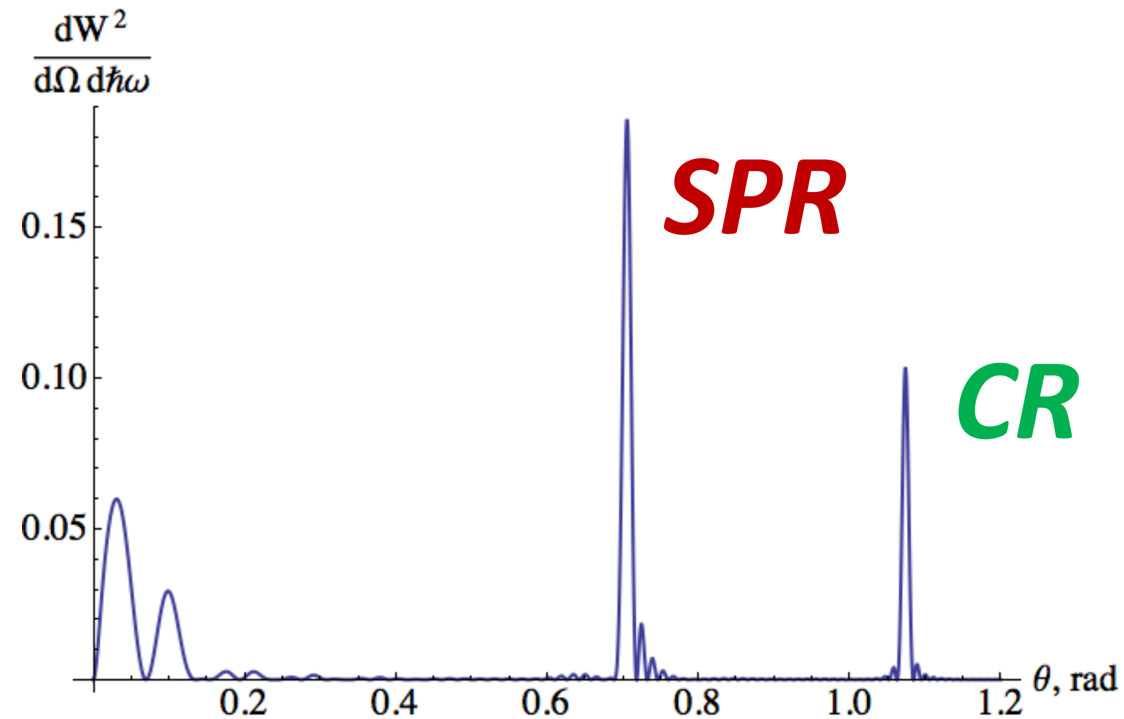

$\lambda = 0.6\ mm$

$d = 2l$

$a = 0.1\ mm$

$N = 60$

$\gamma = 16$

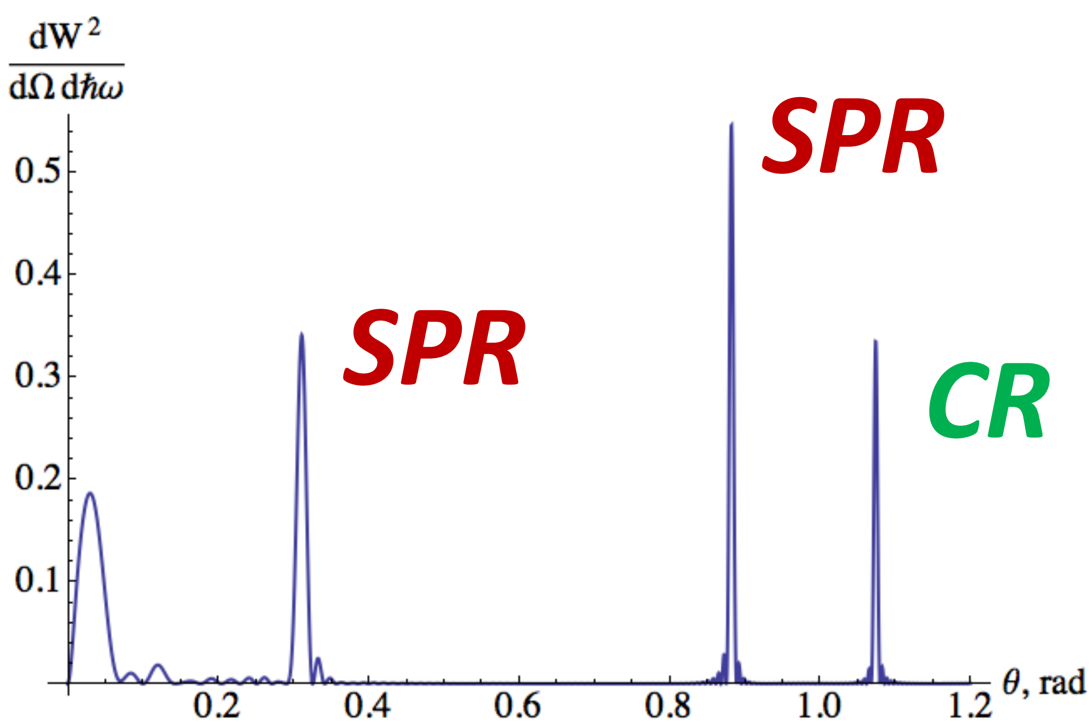

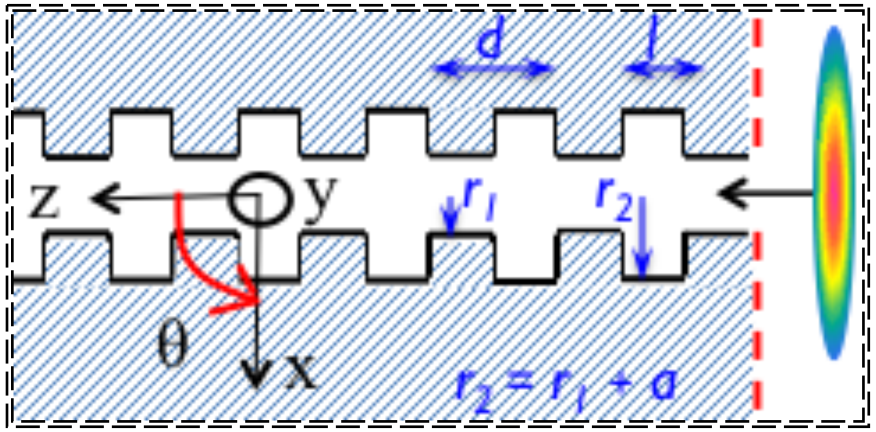

Numerical optimization

$$f = F(x_1, \dots, x_i)$$

$$\left.\begin{array}{l} x_1 \in [a_1, a_2] \\ . \\ x_i \in [a_{i1}, a_{i2}] \end{array}\right\} i = 5 \div 10$$

$$\left\{ x_{1\,\text{optimal}}, \dots\dots\dots, x_{i\,\text{optimal}} \right\}$$

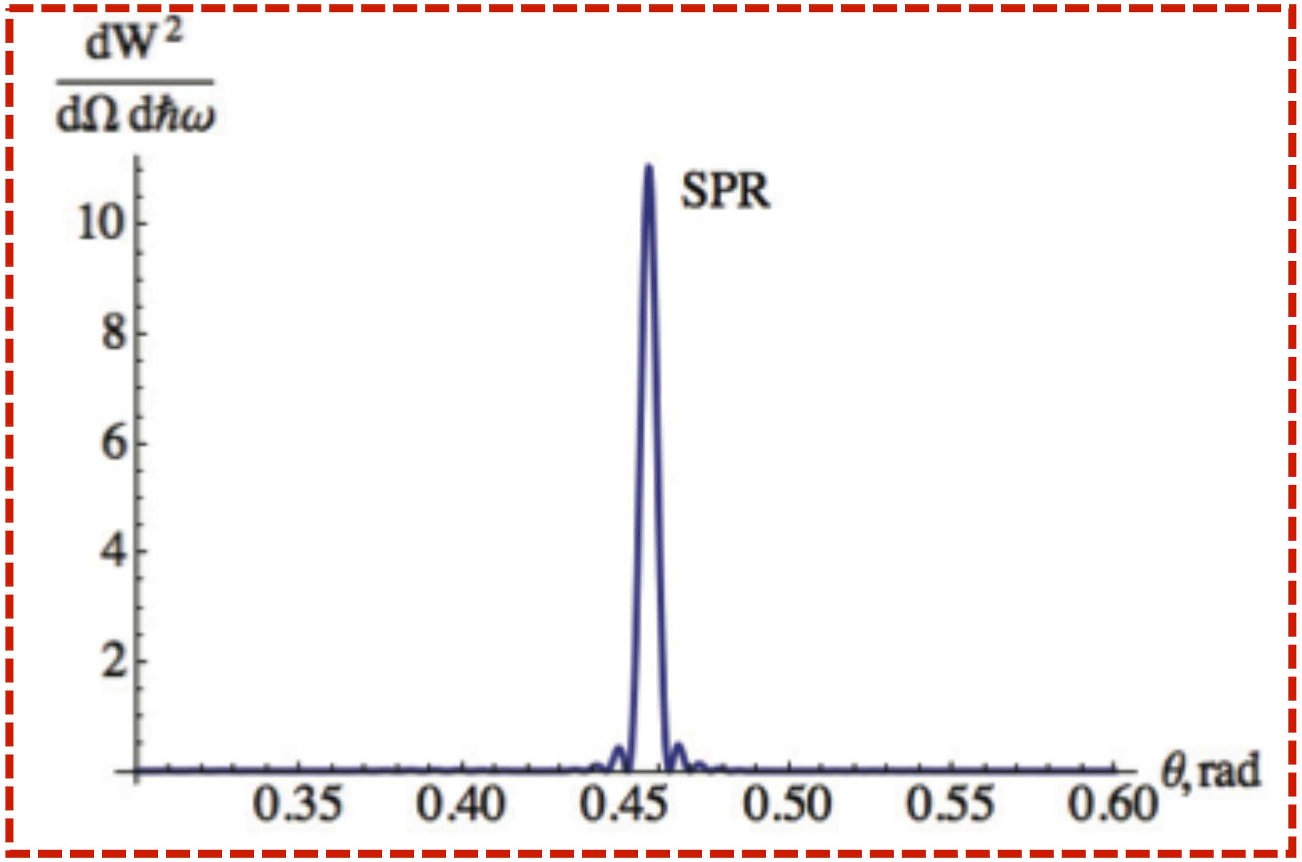

A.A. Ponomarenko, V.M. Sukharev, A.A. Tishchenko, M.N. Strikhanov, Numerical optimization of THz source based on interaction between an electron beam and a dielectric target, Physics Procedia (2015)

Theoretical result №1 – $\mathbf{E}_1(\mathbf{r},\omega)$

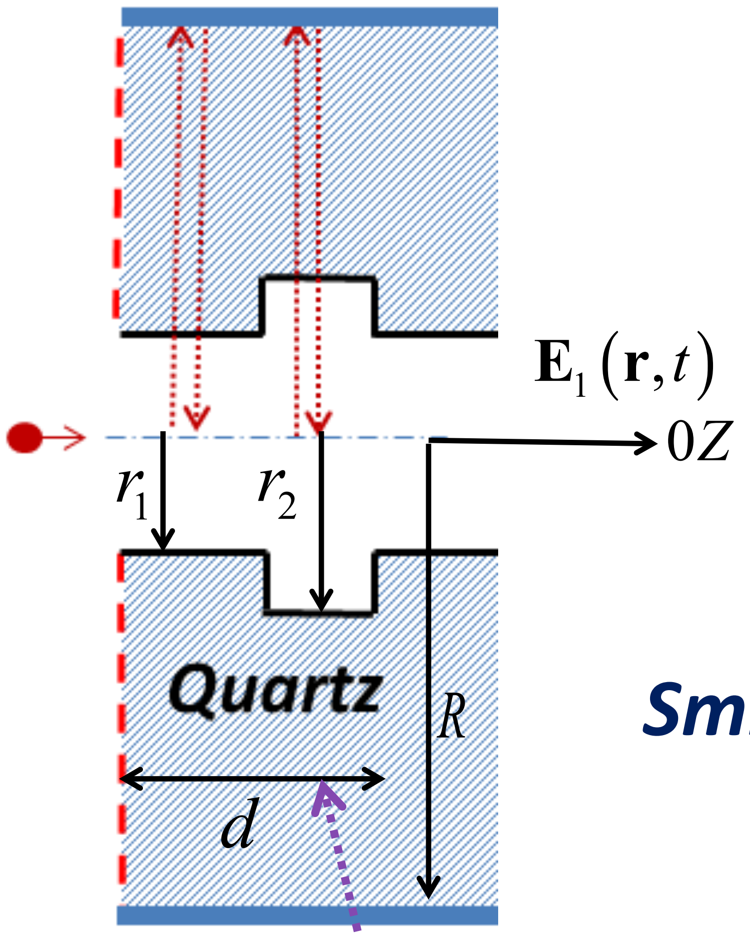

$$\boxed{\mathbf{E}_1(\mathbf{r},t)=\int_{-\infty}^{\infty} d\omega\, e^{-i\omega t}\,\mathbf{E}_1(\mathbf{r},\omega)}$$

$$k=\frac{2\pi}{\lambda}\sqrt{\varepsilon}$$

$$F_1(r)=-k\,r\,J_1(k\,r)K_0\left(\frac{k}{\gamma\beta}r\right)+\frac{k}{\gamma\beta}r\,J_0(k\,r)K_1\left(\frac{k}{\gamma\beta}r\right)$$

$$F_2(r)=k\,r\,J_0(k\,r)K_1\left(\frac{k}{\gamma\beta}r\right)+\frac{k}{\gamma\beta\sqrt{\varepsilon}}r\,J_1(k\,r)K_0\left(\frac{k}{\gamma\beta}r\right)$$

Smith-Purcell

$$\mathbf{E}_1(\mathbf{r},\omega)=i\frac{e(2\pi)^3}{\beta^{-1}}\boxed{\frac{1-e^{-ik\beta^{-1}d\,N}}{1-e^{ik\beta^{-1}d}}}\times$$

$$\times\underline{\mathbf{e}_z}\left(\left(e^{-ik\beta^{-1}l}-1\right)\left(\underline{F_1(r_1)-F_1(R)}\right)+\left(e^{-ik\beta^{-1}d}-e^{-ik\beta^{-1}l}\right)\left(\underline{F_1(r_2)-F_1(R)}\right)\right)\times$$

$$\times e^{-ik(R-r_2)}\left(\underline{e^{-ika}\sum_n\theta(z-nd)\theta(-z+nd+l)+\sum_n\theta(z-nd-l)\theta(-z+(n+1)d)}\right)$$

Theoretical result №1 – $E_1(r,t)$

$$\mathbf{E}_1(r,t)=i\frac{e(2\pi)^3}{\beta^{-1}}\mathbf{e}_z\int_{-\infty}^{+\infty}d\omega\, e^{-i\omega t}\sum_{n'}e^{-2\pi i\frac{\omega}{c}\beta^{-1}d\,n'}\,e^{-2\pi i\,\frac{\omega}{c}(R-r_2)}$$

$$\times\left(\left(e^{-ik\beta^{-1}l}-1\right)\left(F_1(r_1)-F_1(R)\right)+\left(e^{-ik\beta^{-1}d}-e^{-ik\beta^{-1}l}\right)\left(F_1(r_2)-F_1(R)\right)\right)\times$$

$$\times\left(e^{-ika}\sum_n\theta(z-nd)\theta(-z+nd+l)+\sum_n\theta(z-nd-l)\theta(-z+(n+1)d)\right)$$

$\lambda=0.3\ mm$

$l=1\ mm$

$r_1=1\ mm$

$R=2\ mm$

$d=2l$

$a=0.2\ mm$

$N=10$

$\gamma=16$

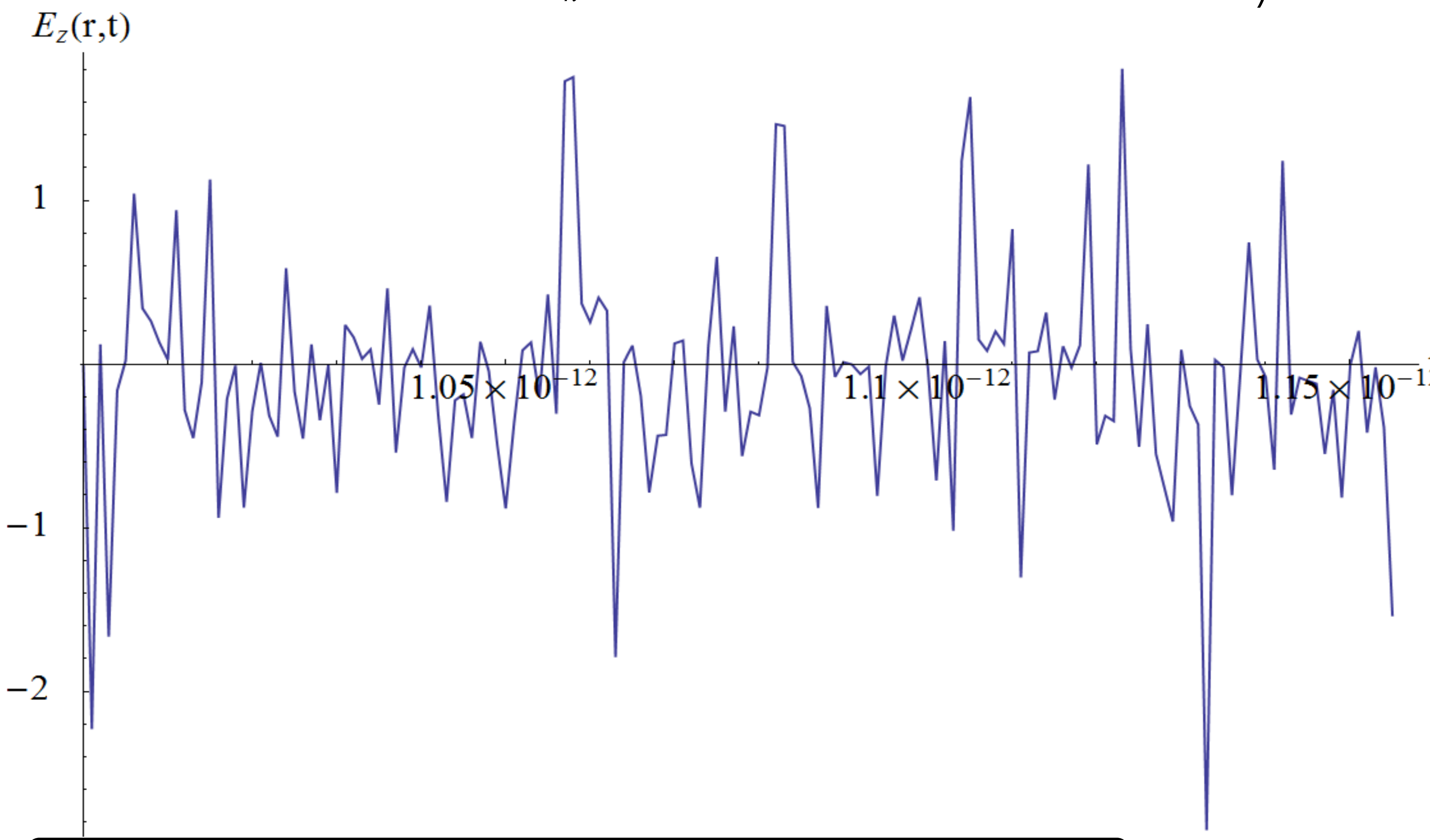

Analysis – $E_l(r)$

$\lambda = 0.3\ mm$

$l = 1\ mm$

$d = 2l$

$a = 0.2\ mm$

$N = 10$

$\gamma = 16$

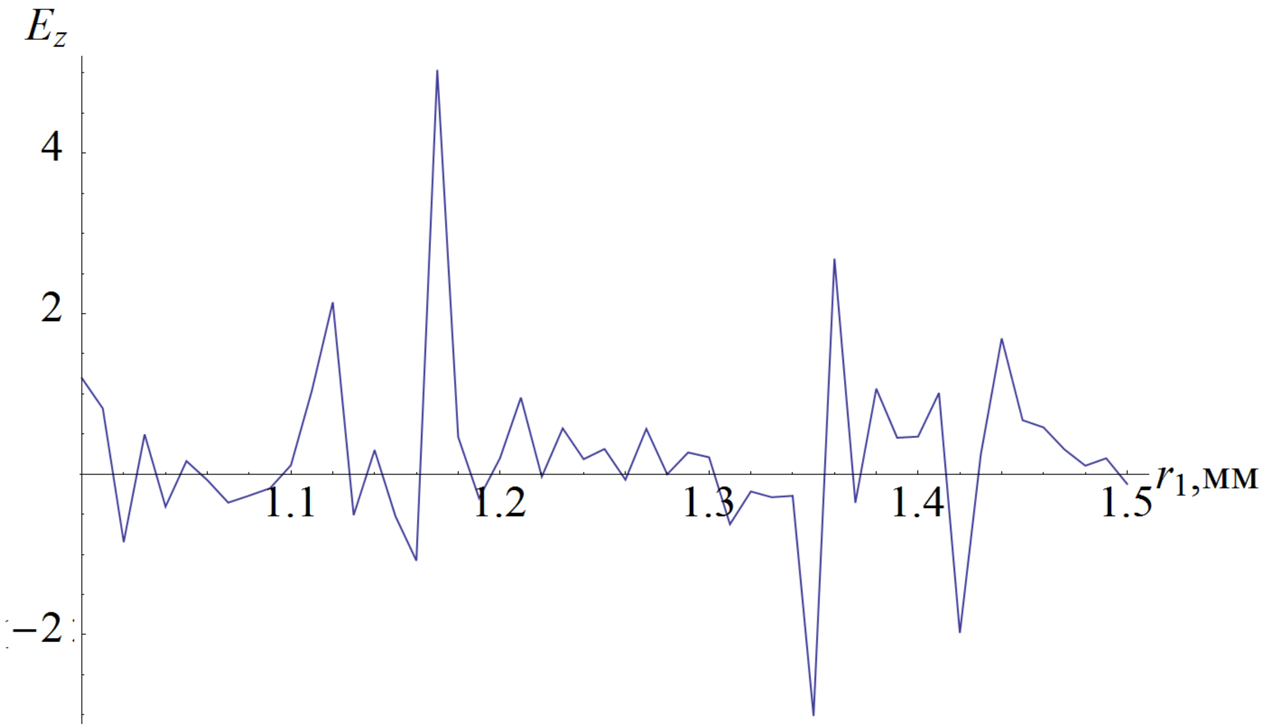

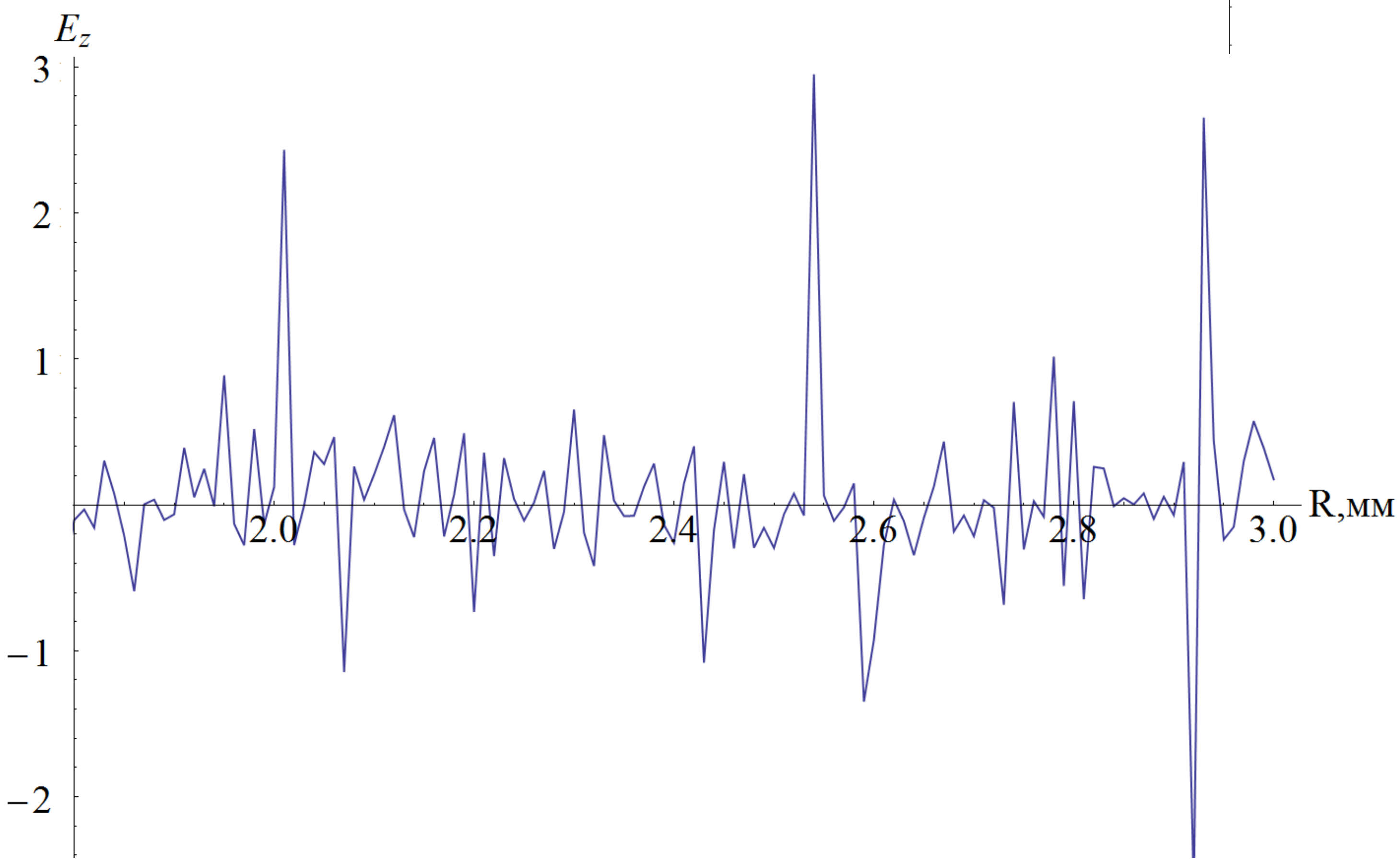

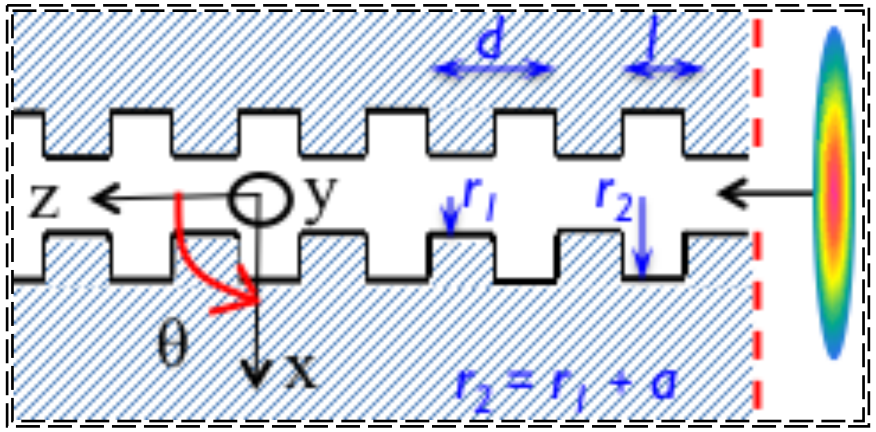

Analysis – $E_l(r)$

$$\lambda = 0.3\ mm$$
$$l = 1\ mm$$
$$d = 2l$$
$$a = 0.2\ mm$$
$$N = 10$$
$$\gamma = 16$$

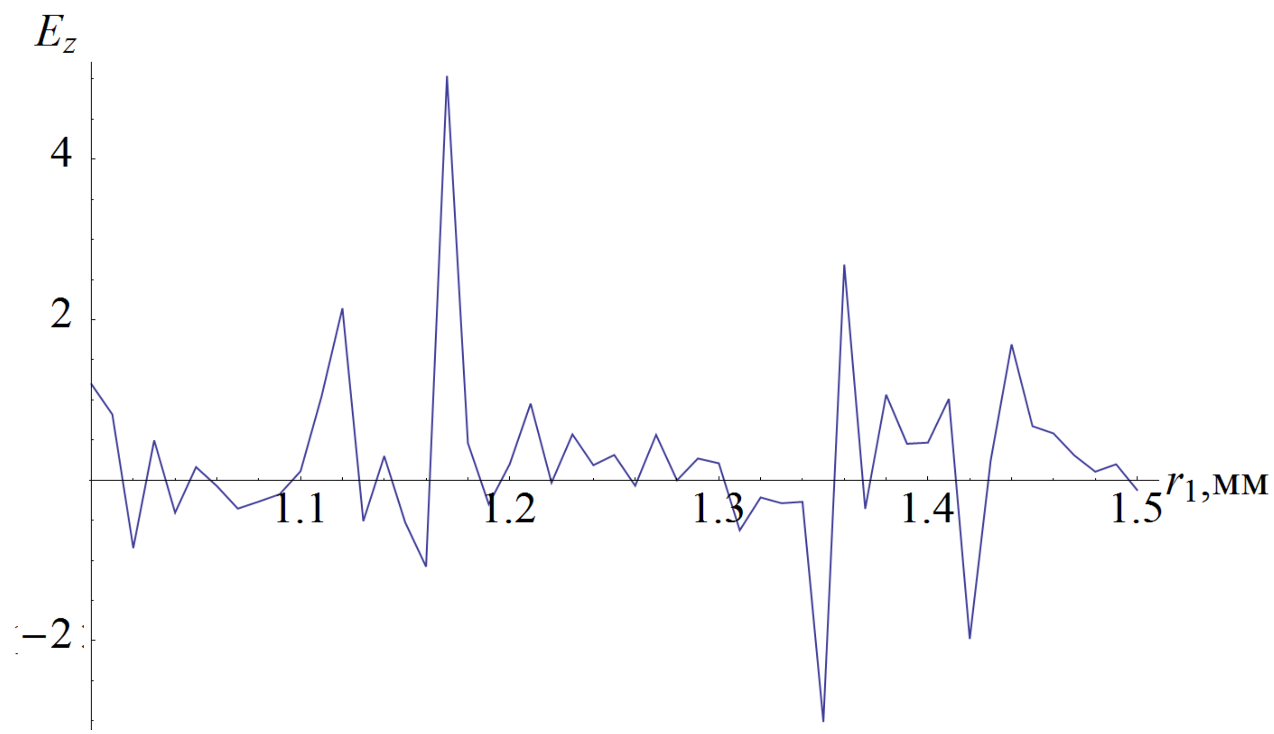

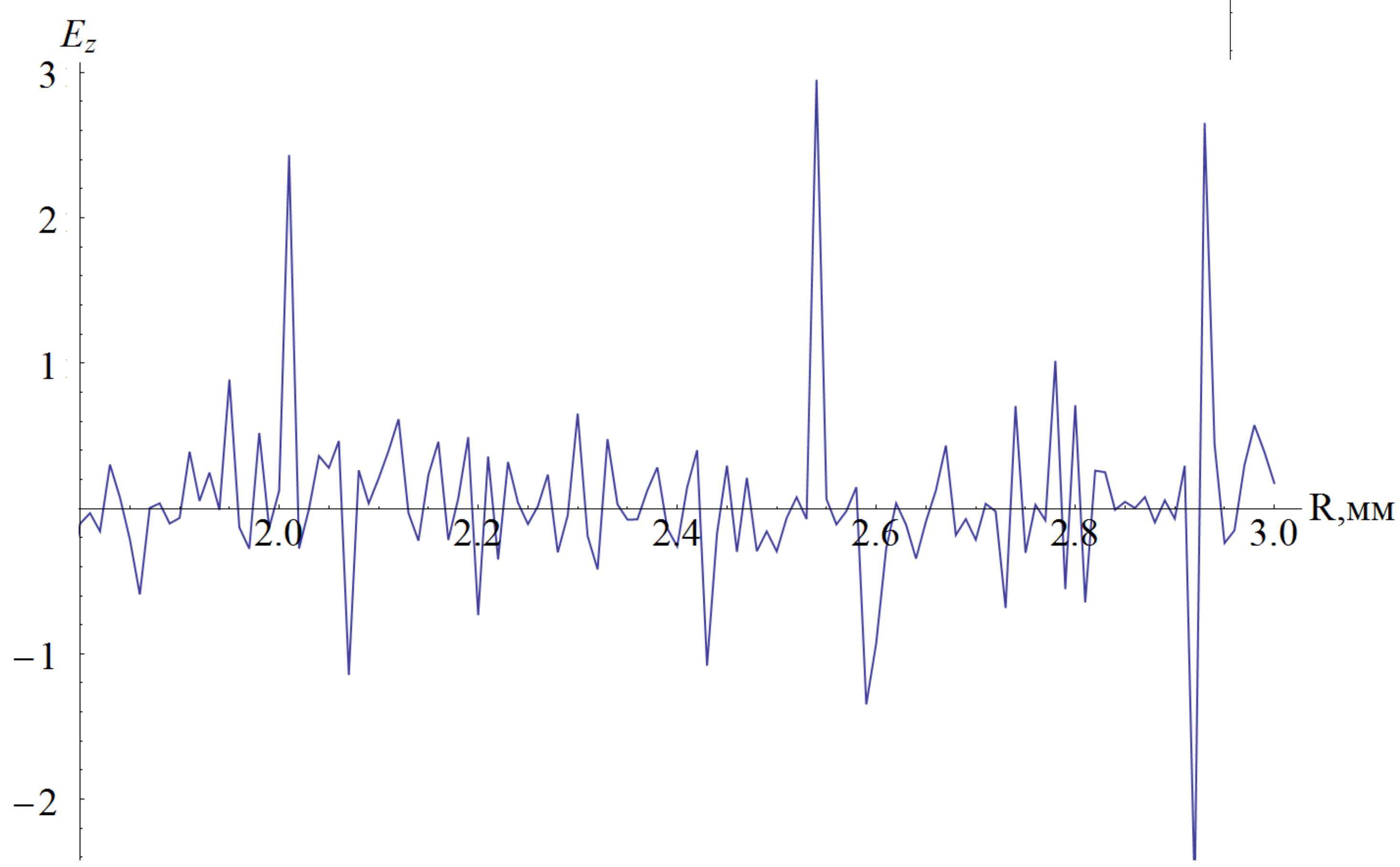

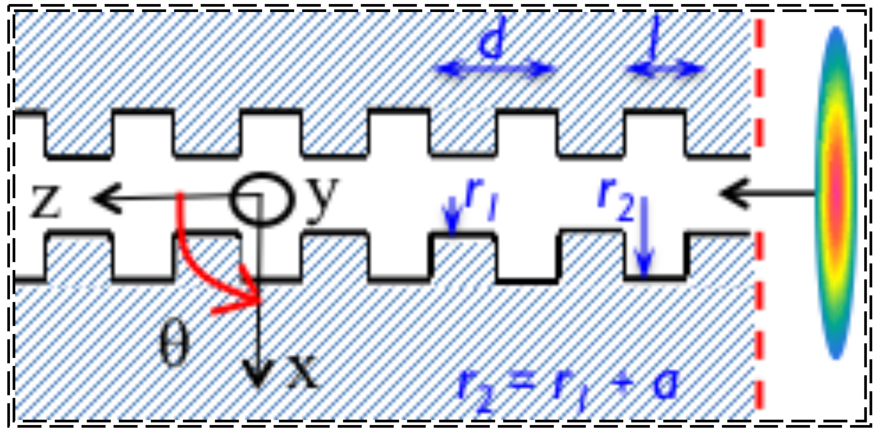

Articles – wakefield acceleration

Radiation of charged particle bunches in corrugated waveguides with small period

A.V. Tyukhtin,[a,1] V.V. Vorobev,[a] E.R. Akhmatova[a] and S. Antipov[b,c]

[a] *Saint-Petersburg State University, 7/9 Universitetskaya nab., St. Petersburg, 199034, Russia*
[b] *Argonne National Laboratory, Argonne, IL 60439 U.S.A.*
[c] *Euclid TechLabs LLC, Solon, OH 44139 U.S.A.*

Russia

USA

PHYSICAL REVIEW ACCELERATORS AND BEAMS **21,** 031302 (2018)

Radiation of a charge flying in a partially loaded dielectric section of a waveguide

Aleksandra A. Grigoreva,[1] Andrey V. Tyukhtin,[1] Viktor V. Vorobev,[1] Sergey N. Galyamin,[1] and Sergey Antipov[2]

[1] *Saint Petersburg State University, 7/9 Universitetskaya nab., St. Petersburg 199034, Russia*
[2] *Euclid Techlabs, 365 Remington blvd, Bolingbrook, Illinois 60440, USA and Argonne National Laboratory, 9700 S. Cass ave, Lemont, Illinois 60439, USA*

(Received 22 November 2017; published 12 March 2018)

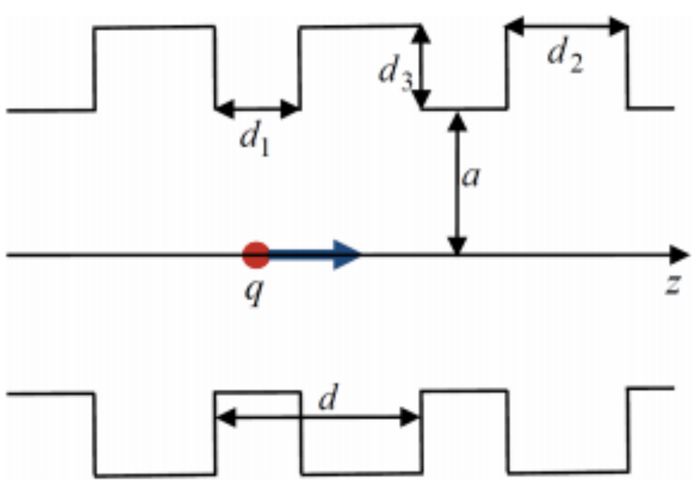

Figure 1. Cross section of the waveguide.

NOT ***SPR !!!***
only ***CR***

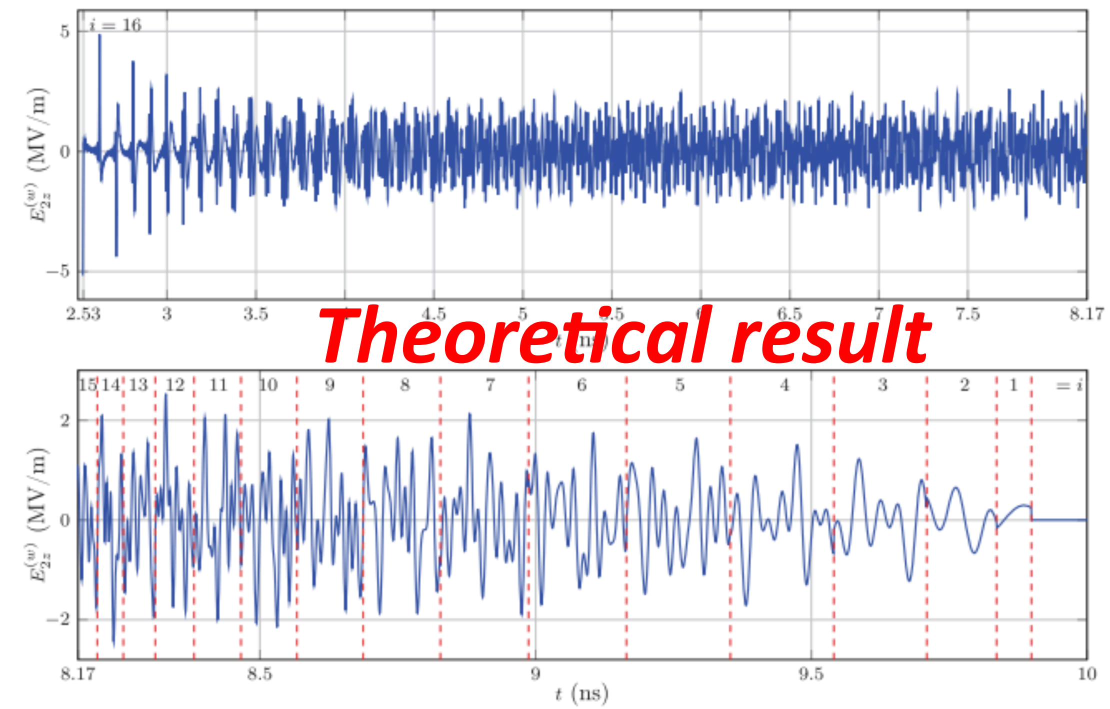

FIG. 2. Dependence of the reduced wakefield longitudinal component $E_{2z}^{(w)}$ on time t at point $r = 0$ cm, $z = 75$ cm (obtained on the basis of analytical results). Waveguide and point charge parameters are $a = 1$ cm, $b = 0.2$ cm, $\varepsilon_d = 4$, $\mu_d = 1$, $q = 1$ nC, $v = 0.99c$. The number i means the number of Cherenkov modes contributing in a corresponding time interval.

CST simulations

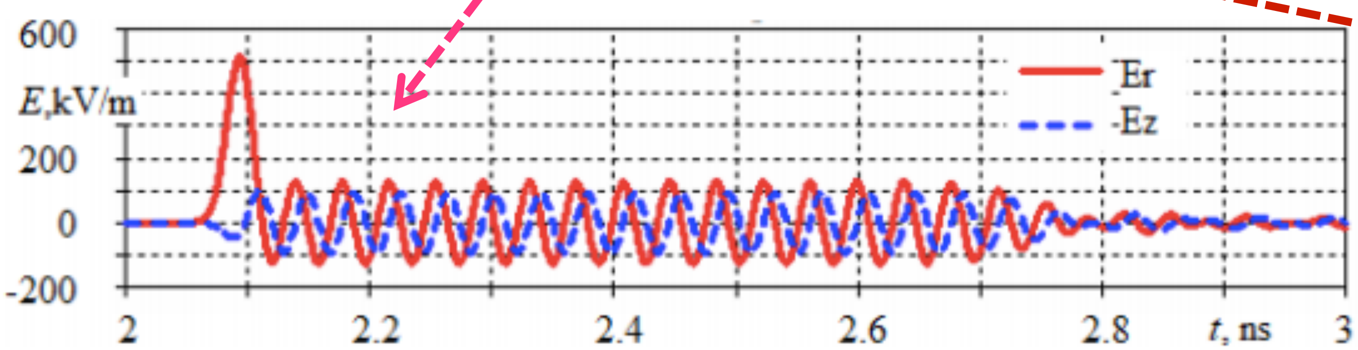

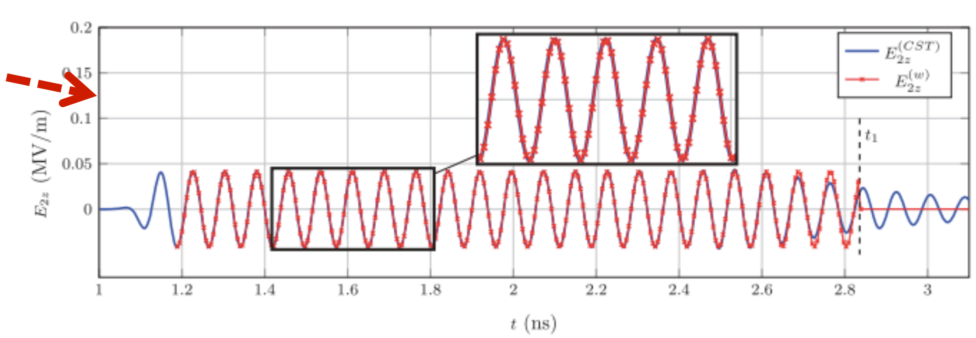

FIG. 4. Dependence of component $E_{2z}^{(CST)}$ of the total field obtained using CST simulation (blue solid line) and reduced wakefield component $E_{2z}^{(w)}$ obtained from analytical investigation (red marked line) on time t at point $r = 0.3$ cm, $z = 30$ cm. Waveguide and bunch parameters are $a = 1$ cm, $b = 0.7$ cm, $\varepsilon_d = 4$, $\mu_d = 1$, $q = 1$ nC, $\sigma = 0.6$ cm, $v = 0.9c$.